Neurotoxicology 70 (2019) 161–179

Contents lists available at ScienceDirect

Neurotoxicology

journal homepage: www.elsevier.com/locate/neuro

Full Length Article

Carbofuran hampers oligodendrocytes development leading to impaired myelination in the hippocampus of rat brain

Brashket Seth[a,b,1], Anuradha Yadav[a,b,1], Ankit Tandon[a,c,1], Jai Shankar[d], Rajnish Kumar Chaturvedi[a,b,*]

[a] Developmental Toxicology Laboratory, Systems Toxicology and Health Risk Assessment Group, CSIR-Indian Institute of Toxicology Research (CSIR-IITR), Vishvigyan Bhavan, 31, Mahatma Gandhi Marg, Lucknow 226001, Uttar Pradesh, India
[b] Academy of Scientific and Innovative Research (AcSIR), CSIR-IITR Lucknow Campus, Lucknow, 226001, Uttar Pradesh, India
[c] School of Dental Sciences, Department of Biochemistry, Babu Banarasi Das University, BBD City, Faizabad Road, Lucknow, 226028, India
[d] Central Instrumentation Facility, CSIR-Indian Institute of Toxicology Research (CSIR-IITR), Vishvigyan Bhavan, 31, Mahatma Gandhi Marg, Lucknow 226001, Uttar Pradesh, India

ARTICLE INFO

Keywords:
Carbofuran neurotoxicity
Hippocampal myelination
Oligodendrogenesis
Neural stem cells
Oligodendrocyte progenitor cells

ABSTRACT

During the mammalian brain development, oligodendrocyte progenitor cells (OPCs) are generated from neuroepithelium and migrate throughout the brain. Myelination is a tightly regulated process which involves time framed sequential events of OPCs proliferation, migration, differentiation and interaction with axons for functional insulated sheath formation. Myelin is essential for efficient and rapid conduction of electric impulses and its loss in the hippocampus of the brain may result in impaired memory and long-term neurological deficits. Carbofuran, a carbamate pesticide is known to cause inhibition of hippocampal neurogenesis and memory dysfunctions in rats. Nonetheless, the effects of carbofuran on OPCs proliferation, fate determination, maturation/differentiation and myelination potential in the hippocampus of the rat brain are still completely elusive. Herein, we investigated the effects of sub-chronic exposure of carbofuran during two different time periods including prenatal and adult brain development in rats. We observed carbofuran hampers OPCs proliferation (BrdU incorporation) and oligodendroglial differentiation in vitro. Similar effects of carbofuran were also observed in the hippocampus region of the brain at both the time points. Carbofuran exposure resulted in reduced expression of key genes and proteins involved in the regulation of oligodendrocyte development and functional myelination. It also affects the survival of oligodendrocytes by inducing apoptotic cell death. The ultrastructural analysis of myelin architecture clearly depicted carbofuran-mediated negative effects on myelin compaction and g-ratio alteration. Conclusively, our study demonstrated that carbofuran alters myelination potential in the hippocampus, which leads to cognitive deficits in rats.

1. Introduction

Myelination is the vital process which provides insulation to axons increasing the speed and efficiency of nerve impulse conductance. Myelin is a fatty sheath composed of modified plasma membrane of specialized glial cells that surrounds the axons (Saab and Nave, 2017). Mature oligodendrocytes are responsible for functional myelination in the central nervous system (CNS), while Schwann cells do myelin formation in the peripheral nervous system (Simons and Nave, 2015). The myelination in rodents occurs at a maximal rate around postnatal day 20 continuing until for at least 16 weeks of age (Doretto et al., 2011; Young et al., 2013). De-myelination of axons undergoes considerable physiological changes that result in axonal dysfunction, degeneration, and loss of sensory and motor functions. There are certain circumstances for progressive de-myelination of axons, which include inhibitory factors promoting cell death among newly generated oligodendrocytes and deficient expression of key growth factors essential for proper myelin synthesis (Alizadeh et al., 2015). The impaired myelination may lead to a variety of neurological deficits and delayed nerve conductance (Nickel and Gu, 2018; Chambers and Perrone-Bizzozero, 2004). Oligodendrocyte progenitor cells (OPCs) are the source of new oligodendrocytes in the brain, which undergo extremely complex and

* Corresponding author at: Developmental Toxicology Laboratory, Systems Toxicology and Health Risk Assessment Group, CSIR-Indian Institute of Toxicology Research (CSIR-IITR), Vishvigyan Bhavan, 31, Mahatma Gandhi Marg, Lucknow 226001, Uttar Pradesh, India.
E-mail address: rajnish@iitr.res.in (R.K. Chaturvedi).
[1] These authors contributed equally.

https://doi.org/10.1016/j.neuro.2018.11.007
Received 5 June 2018; Received in revised form 14 November 2018; Accepted 20 November 2018
Available online 22 November 2018
0161-813X/

tightly controlled sequential events of proliferation, migration and differentiation into myelin-producing cells (de Castro and Bribian, 2005). Defects in oligodendrocyte proliferation and maturation during development may result in demyelinating pathologies, such as multiple sclerosis and schizophrenia (Chambers and Perrone-Bizzozero, 2004; Dutta et al., 2011). The impaired myelination in the hippocampus has been documented in various neurological diseases including autism, anxiety, schizophrenia, multiple sclerosis, epilepsy, Alzheimer's disease and depression (Chambers and Perrone-Bizzozero, 2004; Dutta et al., 2011; Noble, 2004). Environmental exposure of several toxicants such as solvents, xenoestrogen and heavy metals causes developmental abnormalities due to compromised myelination in the CNS (Lee et al., 2010; Brubaker et al., 2009; Rai et al., 2013; Tiwari et al., 2015a). Recently, we found that gestational exposure of Bisphenol-A, a synthetic xenoestrogen and component of plastic polycarbonate baby bottles causes impaired myelination and neurodegeneration in the hippocampus leading to cognitive deficits (Tiwari et al., 2015a; Agarwal et al., 2015).

Carbofuran (2,3-dihydro-2,2-dimethyl-7-benzofuranyl methyl carbamate), is one of the widely known carbamate pesticide and commonly used for pest control in the developing countries. It is non-specific in action that exhibits potential toxicity in both target pests and non-target animal species including the human (Li et al., 2009). It is moderately soluble in water, slightly volatile and has a high potential for leaching to groundwater. The common routes of its exposure involve inhalation, ingestion or absorption through the skin (Gammon et al., 2012). The acute neurotoxicity of carbofuran is associated with its anticholinesterase (AChE) activity inhibiting the neurotransmission due to the accumulation of acetylcholine in synapses (Chahal et al., 2015). The fetal brains are more susceptible to carbofuran toxicity due to their inability to metabolize carbofuran resulting in more prominent AChE inhibition in the fetus than the adult. The lipophilic nature of carbofuran supports its accumulation in fat deposits in different vital organs of the animal system (Gupta et al., 1994). Earlier reports revealed that the neurotoxicity of carbofuran is basically associated with ROS generation and mitochondrial dysfunction in the brain (Kamboj et al., 2008; Gupta et al., 2007). Carbofuran dose-dependently decreases the activity of superoxide dismutase, catalase, and glutathione-S-transferase, subsequently generating the condition of oxidative burst in the brain (Jaiswal et al., 2014). Carbamates interact with SH-groups of various cellular enzymes and affect the assembly of fibrillary proteins like neurofilaments (Schmuck and Mihail, 2004). It causes DNA fragmentation and induces apoptosis resulting in the loss of hippocampal neurons (Gupta et al., 2007). Several other studies showed that carbofuran elicits neurophysiological and neurobehavioral alterations as well as motor deficits in rodents (Kamboj et al., 2006a; Kamboj and Sandhir, 2007; Moser et al., 2010). A recent study also showed that carbofuran causes tau hyper-phosphorylation in the hippocampus inducing Alzheimer's disease-like pathology in the brain (Chen et al., 2012). In our previous studies, we have reported that exposure of carbofuran during gestation causes inhibition of hippocampal neurogenesis and neurodegeneration in the rat offsprings through alterations in TGF-β signaling (Seth et al., 2017; Mishra et al., 2012).

However, whether exposure of carbofuran during different developmental periods of the brain imposes any toxic effects on myelination process in the hippocampus is still elusive. Therefore, in this study, we evaluated the effects of carbofuran exposure during prenatal and postnatal developmental periods on myelination potential by accessing the cellular process of oligodendrogenesis in the hippocampus of rat brain. Here, we demonstrated that carbofuran causes inhibition of OPCs proliferation and differentiation, and induces apoptosis of oligodendrocytes in the hippocampus. We observed that carbofuran causes impaired myelination due to alterations in the expression of genes and levels of proteins involved in the regulation of oligodendrocyte development. Altogether, our results suggest that early gestational and postnatal exposure of carbofuran negatively affects the process of oligodendrogenesis resulting in the impaired axonal myelination in the hippocampus that could lead to learning and memory defects in rats.

2. Materials and methods

2.1. Reagents

Carbofuran (CAS No.1563-66-2), 5′-bromo-2′-deoxyuridine (BrdU) (CAS No. 59-14-3), bovine serum albumin (BSA) (CAS No. 9048-46-8), 3-[4,5-di- methylthiazol-2-yl] 2,5-diphenyltetrazolium bromide (MTT) (CAS No. 298-93-1), Tris-base (CAS No. 77-86-1), poly-L-lysine (PLL) (CAS No. 25988-63-0), basic fibroblast growth factor (bFGF) (CAS No. 106096-93-9), epidermal growth factor (EGF) (CAS No. 62253-63-8), platelet-derived growth factor AA (PDGF-AA) (Cat No. SRP3268), triiodothyronine (T3) (CAS No. 6893-02-3), N-acetyl-L-cysteine (NAC) (CAS No. 616-91-1), N-1 supplement, D-biotin (CAS No. 58-85-5), normal goat serum (NGS), Non-stripped corn oil (CAS No. 8001-30-7) rabbit activated anti-caspase-3 (Cat No. C8487), mouse anti-β-actin (Cat no. A2228), rabbit anti-myelin basic protein (MBP) (Cat No. M3821) and mouse anti-β-Tubulin-III (Cat No. T8578) were procured from Sigma- Aldrich (USA). Neurobasal medium, Hank's balanced salt solution (HBSS), N-2 supplement, B-27 supplement and TRIzol reagent were purchased from Gibco (Invitrogen, USA). Primers were obtained from Integrated DNA Technologies (IDT, USA) and SYBR Green was procured from Applied Biosystems (USA). Anti-fade mounting medium with DAPI was purchased from Vector Labs (Vectashield, Vector laboratories, CA, USA). Culture wares were obtained from Nunc (Denmark). SuperScript first-strand complementary DNA (cDNA) synthesis kit, fluoromyelin stain and Alexa Fluor 488 and Alexa Fluor 594 conjugated secondary antibodies were purchased from Molecular Probes (Invitrogen, USA). Chemiluminescent substrate and bicinchoninic acid (BCA) protein assay kit were obtained from Pierce (USA). Mouse anti-BrdU (Cat no. sc-32323) antibody was obtained from Santa Cruz Biotechnology (Santa Cruz, CA, USA). Rabbit anti Olig-2 (Cat No. ab81093), rabbit anti-Myelin proteolipid protein (PLP) (Cat No.ab28486), mouse anti-CNPase (2′3′-cyclic nucleotide 3′-phosphodiesterase) (Cat no. ab6319), mouse anti-MBP (Cat no. ab62631), rabbit anti-S100β (Cat no. ab41548), mouse anti-neurofilament (NF), rabbit anti-Bcl-2 antibody (Cat no. ab196495) and rabbit anti-BrdU antibodies (Cat No. ab152095) were obtained from Abcam, USA. Rabbit anti-platelet-derived growth factor receptor-α (PDGFR-α) (Cat No. 3164S), rabbit anti-Bax (Cat no. 2772S) and rabbit anti-Myelin-associated glycoprotein (MAG) (Cat No. 9043S) antibodies were procured from Cell Signaling Technology (Danvers, MA, USA).

2.2. Animals and treatment

Adult male and female albino rats of Wistar strain were obtained from animal breeding colony of the CSIR-Indian Institute of Toxicology Research. The animals were housed in polypropylene cages with stainless steel lids under standard animal house conditions of 12 h light/dark cycle and ambient temperature of 25 ± 2 °C. Animals had *ad libitum* access to pellet diet and drinking water. The Institutional Animal Care and Ethics Committee approved all experimental protocols applied to animals throughout the study. The female rats were kept at random mating with males rats and their pregnancy was confirmed by vaginal smear test. The pregnant dams and their pups were randomly segregated into the following groups:

I *PND21 control group:* Received daily single oral gavage of vehicle (corn oil) from gestational day 7 (GD7) to postnatal day 21(PND21).
II *PND21 carbofuran-treated group:* Received daily single oral gavage of carbofuran (1 mg/kg body weight) suspended in corn oil from GD7-PND21
III *PND90 control group:* Received daily single oral gavage of vehicle (corn oil) from PND21-PND90.

IV *PND90 carbofuran treated group:* Received daily single oral gavage of carbofuran (1 mg/kg body weight) suspended in corn oil from PND21–PND90.

The dose of carbofuran (1 mg/kg body weight) was selected on the basis of our previous studies, in which carbofuran caused inhibition of the hippocampal neurogenesis and neurobehavioral alterations in rats (Seth et al., 2017; Mishra et al., 2012). To study the effects of carbofuran during prenatal development, we treated pregnant rats during GD7-PND21 (during gestational and lactational period; total 36 days). The litter size varied from 8 to 12 pups among different dams. Culling of pups was carried out following the standard procedure - 4 Male: 4 Female (Agnish and Keller, 1997). For postnatal studies, we treated 24 male rats with carbofuran from PND21 to PND90, as myelination process continues and approaches at its peak during this period (Doretto et al., 2011; Young et al., 2013). Effect of carbofuran on body weight of pregnant and developing rats was recorded weekly (Supplementary Fig. S1). After respective treatments, only male offsprings (PND21) and adult rats (PND90) from control and carbofuran treated groups were sacrificed after 4 h of last dose of carbofuran for neurochemical and immunohistochemical studies. It was ensured that one pup from each mother was taken for a specific parameter from each group (n = 6 means 1 pup each from 6 different litter per group).

2.3. Oligodendrocyte progenitor cell culture from neural stem cells (NSCs)

NSCs were isolated from the hippocampus region of rat embryos from three different pregnant rats (embryonic day 12) and cultured as described in our earlier studies (Seth et al., 2017; Mishra et al., 2012; Agarwal et al., 2016; Tiwari et al., 2015b). NSCs were cultured in NSC proliferation media comprising neurobasal medium supplemented with 2 mM L-glutamine, 1% antibiotic-antimycotic, 2% B-27, 1% N-2 supplement, EGF (20 ng/ml) and bFGF (20 ng/ml). After 7 days of neurosphere formation, the cells were subjected to induce oligosphere formation by replacing the medium with low concentration of EGF (10 ng/ml) and bFGF (10 ng/ml) following earlier published methods (Fu et al., 2007; Preston et al., 2013). The cultures were fed every 2 days by replacing one-third volume of NSC medium with fresh OPC proliferation medium containing (neurobasal media supplemented with 0.1% BSA, PDGF-AA (10 ng/ml), bFGF (10 ng/ml), 1% B-27, 1% N-1 supplement, and 10 nM D-biotin). With time, the majority of cells migrated out from the neurospheres and attached to the bottom of flask. The adhered cells with bipolar and tripolar process showed morphological characteristics of OPCs. To enhance the purity and vitality of the attached OPC-like cells, the entire medium was replaced with fresh OPC medium. The cultures were allowed to proliferate until visible spheres, referred as oligospheres had formed. The characterization of oligospheres derived from hippocampal NSCs was performed using OPC markers Olig-2 and PDGFR-α (Fig. 1a). The generated oligospheres were passaged and transferred to PLL-coated chamber slides containing OPC differentiation media (neurobasal medium supplemented with 0.1% BSA, 1% B-27, 1% *N*-1 supplement, *N*-acetyl-L-cysteine and 30 nM tri-iodothyronine) for differentiation-related experiments (Tiwari et al., 2015a).

2.4. Myelinating neuron-OPCs Co-cultures

Hippocampal neurons were isolated from rat embryos (embryonic day 12) and cultured on PLL-coated chamber slides as described (Seibenhener and Wooten, 2012; Brewer and Torricelli, 2007). Briefly, cells were cultured in the presence of 5 μM cytosine arabinoside (AraC) to eliminate non-neuronal cells in neuronal media containing 1% B-27, 1% N-2 supplement and 2 mM L-glutamine (Seibenhener and Wooten, 2012). Neurons were fed every 2 days by removing half of the old media and replacing it with the same volume of fresh media. After 7 days of neuron culture, hippocampus-derived rat OPCs were then plated onto hippocampal neurons in the presence of OPC differentiation media and treated with 50 μM carbofuran or DMSO as a vehicle (Zhang et al., 2011). The co-cultures were allowed to grow for the next 3 days and then fixed cells with 4% paraformaldehyde for immunocytochemical analysis.

2.5. MTT assay for cell viability

In order to analyze the effect of carbofuran on cell viability of OPCs, MTT assay was performed following the method used in our earlier studies (Tiwari et al., 2015b; Seth et al., 2017). Briefly, cells were seeded in 96 well plate (1×10^4 cells/well) and exposed with different concentrations of carbofuran (1, 10, 20, 50, 100, 200 and 400 μM). After incubation of 24 h, 20 μl of MTT (5 mg/ml stock solution in PBS) was added to every well containing cells in 200 μl medium, and the cultures were allowed to incubate at 37 °C for next 4 h. After incubation medium was carefully taken out and resulting formazan crystals formed were solubilized in DMSO (200 μl/well). Absorbance was measured at 570 nm using a Multiwell microplate reader (Synergy HT, Bio-Tek, USA). The results were calculated in terms of cell viability as a percent of vehicle control.

2.6. Oligosphere growth kinetic assay

We performed oligosphere growth kinetics assay to evaluate the effects of carbofuran on proliferation of OPCs and aggregate formation following earlier published studies (Vitry et al., 1999; Tiwari et al., 2015a). In brief, single-cell suspension of the hippocampal-derived OPCs was seeded in a 12-well plate at a density of 5×10^4 cells/well in OPCs proliferation medium and exposed with different concentrations of carbofuran (1, 10, 50, 100, 200, and 400 μM) and DMSO as vehicle for 72 h. The images of round oligospheres in all the groups were captured using a Nikon Eclipse Ti-S inverted phase contrast microscope. The total number of oligospheres was counted per well in each group and the diameter of randomly selected 10 oligospheres in each group was measured using ImageJ software (NIH).

2.7. BrdU incorporation and immunocytochemistry

To evaluate the effects of carbofuran on proliferation and differentiation of OPCs in culture, immunocytochemistry was performed. In brief, oligospheres were harvested by centrifugation at 1000 rpm and dissociated into single-cell suspension using 0.25% trypsin followed by neutralization with soybean trypsin inhibitor. Dissociated OPCs were plated on poly-L-Lysine coated 4-well chamber slide at a density of 10,000 cells per well containing OPC proliferation medium for proliferation-related experiments (e.g., PDGFR-α and Olig-2 labeling). The cells were exposed with non-cytotoxic concentration of carbofuran (50 μM) for 24 h and the cells were also pulsed with 10 μM BrdU for 12 h before fixation with 4% paraformaldehyde. For differentiation studies (e.g., MBP, CNPase labeling), OPCs were first seeded in proliferation medium and pulsed with 10 μM BrdU for 12 h before switching to differentiation medium. The cells were then treated with carbofuran (50 μM) for 48 h followed by fixation with 4% paraformaldehyde and processed for immunocytochemistry. For BrdU incorporation analysis, cells were treated with 2 N HCl after fixation for 10 min at 37 °C to denature DNA followed by neutralization with borate buffer (0.1 M, pH 8.5) for 10 min at room temperature. Cells were then blocked with 3% NGS, 0.5% BSA, and 0.1% Triton X-100 in PBS for 60 min. The cells were subsequently incubated with following primary antibodies overnight at 4 °C diluted in blocking solution; BrdU (1:200), Olig-2 (1:200), PDGFR-α (1:100), MBP (1:200), CNPase (1:250), MAG (1:250) and NF (1:50). The cells were then incubated with a mixture of Alexa 488 and 594 conjugated secondary antibodies (1:400) for 2 h at room temperature followed by washing 3 times with PBS. The slides containing cells were cover-slipped with DAPI including mounting medium and analyzed under an inverted fluorescent microscope

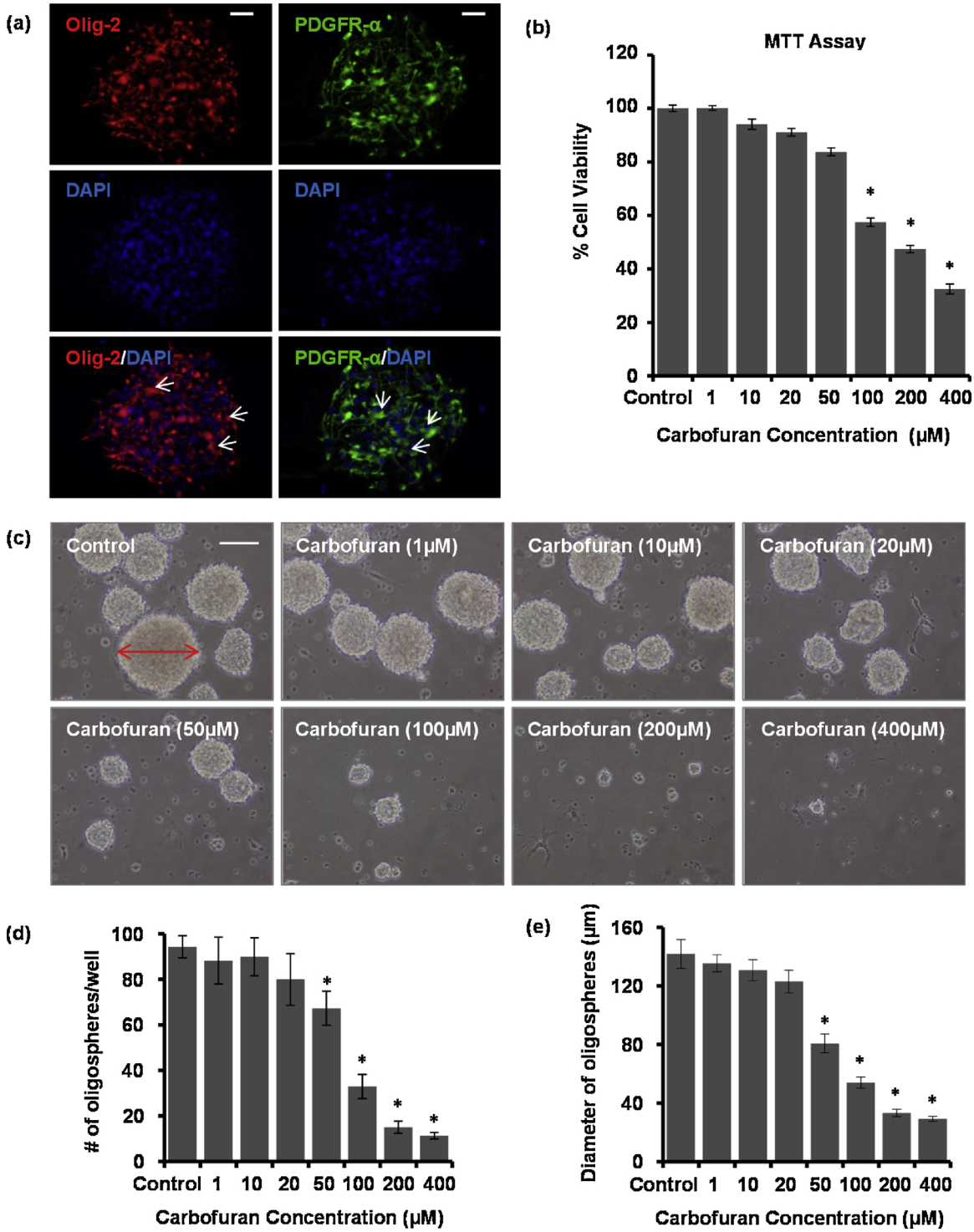

Fig. 1. Carbofuran reduces viability and proliferation of the hippocampal derived OPCs in vitro. (a) Characterization of NSCs derived oligospheres was performed showing expression of markers of oligodendrocytes progenitor cells (OPCs). Oligospheres were immunostained with OPCs markers Olig-2 (red) and PDGFR-α (green) and counterstained with nuclear stain DAPI (blue). Nearly 97% DAPI positive cells were labeled with Olig-2 or PDGFR-α reflecting highly purified OPCs culture. (b) Cell viability of OPCs was evaluated by MTT reduction assay. OPCs isolated from the hippocampus were seeded in 96-well plates and treated with varying concentrations of carbofuran and DMSO as a vehicle for 24 h. Graph showing percent cell viability in terms of MTT reduction at various concentrations of carbofuran. (c) Oligosphere growth kinetics assay was used to study the effects of carbofuran on total count and the mean diameter of oligospheres cultured until 3 days in vitro. Representative phase contrast photomicrographs of oligospheres formed from the OPCs treated with different concentration of carbofuran. (d–e) Graph representing the total count and the mean diameter of oligospheres in all the experimental groups. Values are mean ± SEM (n = 3 independent experiments), *$p < 0.05$ vs control. Scale bar = 20 μm in (a) and 100 μm in (c). (For interpretation of the references to colour in this figure legend, the reader is referred to the web version of this article.)

equipped with NIS Elements BR imaging software. The total number of co-labeled cells was counted per well in each group.

2.8. Immunohistochemistry for cell phenotype analysis

After respective treatments, rats were deeply anesthetized with ketamine and xylazine mixture (3:1) and transcardially perfused with PBS followed by 4% paraformaldehyde. The brains of 6 rats per group were collected and post-fixed overnight in 4% paraformaldehyde and then transferred to a gradient of sucrose (10, 20, and 30% in PBS). 30 µm thin serial coronal sections encompassing the entire hippocampus were sliced using a freezing microtome (Slee Mainz Co., Germany). Sections were kept in citrate buffer at 60 °C for 20 min for antigen retrieval followed by blocking with 3% NGS, 0.5% BSA, and 0.1% Triton X-100 for 2 h. Sections were then probed with primary antibodies rabbit anti-Olig-2 (1:250), rabbit anti-PDGFR-α (1:200), rabbit anti-MBP (1:200), mouse anti-NF (1:50), rabbit anti-MAG (1:250), rabbit cleaved caspase-3 (1:400) for 24 h at 4 °C. After washing thrice with PBS, sections were then incubated with an appropriate combination of species-specific Alexa Fluor-conjugated secondary antibodies for 2 h at room temperature. Sections were mounted on gelatin-coated slides with DAPI containing anti-fade mounting medium. The fluorescence images were captured using a Nikon Eclipse Ti-S inverted fluorescent microscope and analyzed with NIS Elements BR imaging software (Nikon, Japan) as described earlier (Mishra et al., 2012; Agarwal et al., 2016; Tiwari et al., 2015a,c).

2.9. Fluoromyelin staining

The distribution of myelin content in the hippocampus was analyzed using fluoromyelin stain. The staining was performed as per manufacturer's protocol. In brief, brain sections were permeabilized with 0.2% Triton X-100 in PBS for 20 min. Sections were washed thrice in PBS and then incubated with FluoroMyelin stain (1:300 in PBS) for 20 min at room temperature. After rinsing 3 times with PBS, sections were then mounted on glass slides with anti-fade DAPI containing mounting medium and visualized under an inverted fluorescence microscope. The intensities of fluoromyelin stained sections were measured in the images captured at the same gain and exposure time using ImageJ software 1.46r (NIH).

2.10. Immunoreactivity and cell quantification in the hippocampal sections

The quantification of immuno-labeled cells in the hippocampus region of 6 rats per group was carried out following our earlier studies (Mishra et al., 2012; Agarwal et al., 2016). In brief, unbiased stereological methods were applied, where a person without knowledge of the experimental design carried out cell quantification on coded slides. Labeled cells were counted in every sixth section in one in six series, with a total of six sections per rat analyzed. The immunoreactivity of MBP, NF and MAG was measured in six fields of each section of the hippocampus and data were expressed as percent integrated optical intensity as described earlier (Chambers and Perrone-Bizzozero, 2004). The relative immunofluorescence intensity of a specific marker was quantified using ImageJ software (NIH). Co-localization of two different markers was quantified by analysis of Manders co-efficient using JACoP plugin in ImageJ software (NIH). The same perfused brains were used for all the ex vivo measures.

2.11. Gene expression by qReal-Time PCR

The effects of carbofuran on the expression of genes regulating oligodendrocyte development and myelination were examined by quantitative real-time PCR (qRT-PCR). Total RNA from the hippocampal tissue of each group was extracted using Trizol reagent (Invitrogen). The quality and quantity of RNA were determined using NanoDrop spectrophotometer. Cut-off values of > 1.8 (OD260/280) and > 2.0 (OD260/230) were used as quality measures of RNA samples. RNA integrity was analyzed by using denaturing gel electrophoresis. Equal amount of RNA was reverse transcribed to cDNA using SuperScript first-strand cDNA synthesis kit with Oligo-dT. The qRT-PCR was performed with SYBR Green Master Mix using ABI Prism 7900 Sequence Detector System (PE Applied Biosystems; Foster City, CA). The expression of cellular house-keeping gene β-actin served as a control to normalize values. Relative gene expression in terms of fold change was calculated using $2^{-\Delta\Delta Ct}$ method. The details of sequences for primers used in this study are listed in supplementary material (Supplementary Table 1).

2.12. Protein levels analysis by Western blotting

The hippocampus tissues isolated from each group were lysed in a lysis buffer containing protease and phosphatase inhibitors. The protein concentration in each sample was estimated using bicinchoninic acid (BCA) protein assay kit. An equivalent amount of protein (60 µg) from each sample was resolved on SDS-polyacrylamide gel and transferred to PVDF membranes. The membranes were blocked in Western blocker solution for 2 h at room temperature followed by incubation overnight with primary antibodies β-actin (1:10,000), Olig-2 (1:1000), PDGFR-α (1:1000), MBP (1:1000), MAG (1:1000), myelin proteolipid protein (PLP, 1:1000), CNPase (1:1000), Bax (1:2000), Bcl-2 (1:2000) and cleaved caspase-3 (1:1000) at 4 °C. Following three times washing with Tris buffer saline (TBS) + 0.05% Tween-20, membranes were then incubated with horseradish peroxidase-conjugated secondary antibodies (1:5000) for 2 h at room temperature. The protein bands on membrane were detected using a chemiluminescent substrate. The optical density of protein bands was measured by Image J software (NIH, USA). Normalization of the results was done by using β-actin as normalizer.

2.13. Transmission electron microscopy (TEM)

We examined ultrastructural changes in myelin sheath assembly in the hippocampus of rats by TEM. The anesthetized rats were perfused with pre-chilled PBS followed by a mixture of 4% paraformaldehyde and 0.2% glutaraldehyde in PBS (pH 7.4) *via* a cardiac catheter. The brain was excised and small pieces of the hippocampus were immersed in 2.5% glutaraldehyde in 0.1 M sodium cacodylate buffer overnight at 4 °C, followed by post-fixation with OsO4 for 2 h at room temperature. The tissue was dehydrated using acetone gradient (10–100%) and embedded in an Araldite and dodecenyl succinic anhydride mixture and baked at 65 °C for 48 h to prepare blocks. Ultra-thin sections were stained with uranyl acetate and lead citrate and examined under TEM (FEI, Technai G2 Spirit TWIN, USA) equipped with a Gatan digital CCD camera. The g-ratio of axons was determined in randomly selected hundred axons from three sections each of 6 rats per group and calculated as a ratio of the diameter of an axon over the diameter of associated myelin sheath by using ImageJ software as described earlier (Liu et al., 2012).

2.14. Conditioned avoidance response

Neurobehavioral alterations due to postnatal carbofuran exposure in the rats of PND90 groups were assessed in terms of learning and memory functions using a shuttle-box apparatus (Columbus Instruments) (Tiwari et al., 2015c, 2014). Each trial consisted of an electric buzzer (for 5 s) as a conditioned stimulus, followed by of unavoidable foot shock (0.5 mA up for 10 s) to the rats. Each animal was subjected to 20 trials per day repeatedly for consecutive days. The percentage of CAR was considered as the measure of cognitive ability for interpretation of learning and memory. The learning was performed using 6 rats per group for consecutive 3 days from PND80-PND82. A comparison was made between carbofuran treated rats and control rats

on the third day when learning or retention ability in control rats reached ≥90% CAR. The rats were left for 1 week and CAR was measured at PND 90 in both the groups for assessment of memory. The behavioral testing was performed after 4 h of each day's daily dose. The learning and memory in treated rats were calculated as compared to % control. As the normal eyelid opening in rat offspring takes place around at PND14 and ocular structures such as cornea and retina are also underdeveloped at this age and attain their maturity after PND21 (Vrolyk et al., 2018). Thus, the neonatal rats of PND21 groups were not used for this test.

2.15. Statistical analysis

Statistical analysis was performed using GraphPad InStat statistical analysis software version 3.05 for Windows (SanDiego, CA, USA). Comparison of least significant differences among the two groups was determined using unpaired Student's *t*-test by taking t values for error and keeping degrees of freedom at the 5% level of significance and 95% confidence interval. All values were represented as mean ± SEM. Values of $p < 0.05$ were considered statistically significant.

3. Results

3.1. Carbofuran decreases proliferation and differentiation of OPCs in vitro

In this study, the viability of OPCs derived from rat hippocampus incubated with different concentrations of carbofuran (1, 10, 20, 50, 100, 200 and 400 μM) was investigated using MTT assay. The data demonstrated that carbofuran reduced cell viability of OPCs in a concentration-dependent manner (Fig. 1b). Carbofuran did not cause significant alteration in MTT reduction at lower concentrations (1–50 μM). The treatment of carbofuran for 24 h significantly decreased the viability of OPCs at all the concentrations more than 50 μM (Fig. 1b). Here, we found 50 μM concentration of carbofuran as a non-cytotoxic, which was further used to assess the effects of carbofuran in all in vitro experiments. This result is consistent with our earlier reports in which carbofuran reduced the viability of primary NSCs in a similar fashion (Seth et al., 2017). Changes in the number and size of oligospheres are strong qualitative and quantitative indicators in a proliferation assay. An increase in carbofuran concentration caused a significant decrease in total number of oligospheres and mean diameter of oligospheres. A dose-dependent decrease of average mean diameter of oligospheres was observed due to carbofuran treatment, but the values were significant from ≥50 μM concentration as compared with the control group (Fig. 1c–e).

Next, BrdU incorporation assay was performed to study the effects of carbofuran on OPCs proliferation. We found that BrdU incorporation in Olig-2 and PDGFR-α expressing OPCs was significantly reduced by the non-cytotoxic concentration of carbofuran (50 μM) as compared to control. Olig-2, a basic helix loop helix (bHLH) transcription factor, is expressed in OPCs in the developing and mature vertebrate CNS (Wegener et al., 2015). While PDGFR-α is predominantly expressed on the membrane surface of oligodendrocyte precursors and most abundantly used as a marker for OPCs (Pituch et al., 2015). We observed a significant reduction in the count of PDGFR-α/BrdU$^+$ and Olig-2/BrdU$^+$ cells after carbofuran treatment ($p < 0.05$) (Fig. 2a–d). The results from BrdU incorporation assay indicated anti-mitogenic effects of carbofuran on OPCs proliferation.

Next, in order to evaluate the effects of carbofuran on differentiation and maturation of OPCs, we carried out immunocytochemical analysis for expression of markers of oligodendrocyte differentiation (Fig.3). Carbofuran mediated effects on the differentiation of OPCs was assessed by BrdU labeling of MBP$^+$ and CNPase$^+$ cells in culture conditions. Here, we used MBP and CNPase as markers of mature oligodendrocytes. We found that treatment of carbofuran significantly (*$p < 0.05$) reduced the number of MBP/BrdU$^+$ (Fig. 3a, b) and CNPase/BrdU$^+$ cells (Fig. 3c, d) as compared to control. We also observed that the CNPase$^+$ cells contained fewer processes following carbofuran treatment as compared to control group. Interestingly, carbofuran enhanced the number of S100β/BrdU$^+$ cells as compared to control suggesting increased astroglial fate commitment of OPCs in vitro (Fig. 3e, f).

Next, we co-cultured oligodendrocytes with neurons isolated from the hippocampus of rat embryos. We found that carbofuran alters myelination potential of oligodendrocytes as assessed by decreased co-labeling of MBP/NF$^+$ cells as compared to control (*$p < 0.05$) (Fig. 4a, b). We also observed a significant decrease in the number of β-Tubulin$^+$ (mature neuronal marker) cells that were co-labeled with myelinating oligodendrocyte marker MAG following carbofuran treatment in co-culture conditions (Fig. 4c, d). The results from these experiments suggested that carbofuran decreases proliferation and differentiation/maturation of OPCs thereby altering myelination potential of oligodendrocytes in vitro.

3.2. Carbofuran reduces proliferation and pool of OPCs in the hippocampus of rat brain

The effects of carbofuran exposure during prenatal and postnatal developmental periods on proliferation and pool of OPCs were assessed by immunohistochemical expression of markers of OPCs such as Olig-2 and PDGFR-α in the hippocampus. During the CNS development, OPCs migrate from the neuroepithelium to their final destination sites throughout the brain (de Castro and Bribian, 2005). We found significantly reduced numbers of Olig-2$^+$ cells following carbofuran exposure in the dentate gyrus (DG) region of the hippocampus at both PND21 and PND90 as compared to control (*$p < 0.05$) (Fig. 5a, b). These results reveal that carbofuran inhibits proliferation of OPCs in the hippocampus of rat brain. Moreover, the effects of carbofuran exposure on OPCs population were also assessed by counting PDGFR-α$^+$ cells in the hippocampus. The proliferation of OPCs in the CNS relies heavily on the expression of PDGFR-α (Fruttiger et al., 1999). Quantification of the number of PDGFR-α$^+$ cells showed that OPCs population was significantly fewer in the hippocampus of carbofuran treated rats as compared to controls at both PND21 and PND90 (*$p < 0.05$) (Fig. 5c, d). From these experiments, we concluded that the exposure of carbofuran adversely affects OPCs proliferation that leads to a reduction in the pool of oligodendrocyte progenitors in the brain.

3.3. Carbofuran alters immunoreactivity of fluoromyelin, MBP and MAG in the hippocampus

To assess the effects of carbofuran on myelination, we performed myelin staining on coronal sections encompassing the hippocampus region from all the groups using fluorescent FluoroMyelin stain and antibody against myelin antigen MBP and MAG (McQueen et al., 2014; Payne et al., 2011). We found a significant reduction in the intensities of fluoromyelin staining in the hippocampus due to carbofuran exposure at both the time points *i.e.* PND21 and PND90 as compared to control (*$p < 0.05$) (Fig. 6a, b). The MAG is a transmembrane glycoprotein expressed in oligodendroglial membranes of myelin sheaths (Pronker et al., 2016). We observed a profound reduction in MAG immunoreactivity in the hippocampus region due to carbofuran exposure at both PND21 and PND90 as compared to control (*$p < 0.05$) (Fig. 6c, d).

Next, the effects of carbofuran on MBP immunoreactivity were studied in the CA1, CA3 and DG regions of the hippocampus (Fig. 7). We observed a remarkable decrease in intensity of MBP immunoreactive myelinated fibers present in the CA1, CA3 and DG areas in carbofuran treated groups as compared to control (Fig. 7a, b). Further, we assessed myelin distribution among the myelinated axons of the hilus region of DG by co-labeling of MBP and NF (marker of axon caliber). We observed a significant decrease in co-localization of MBP

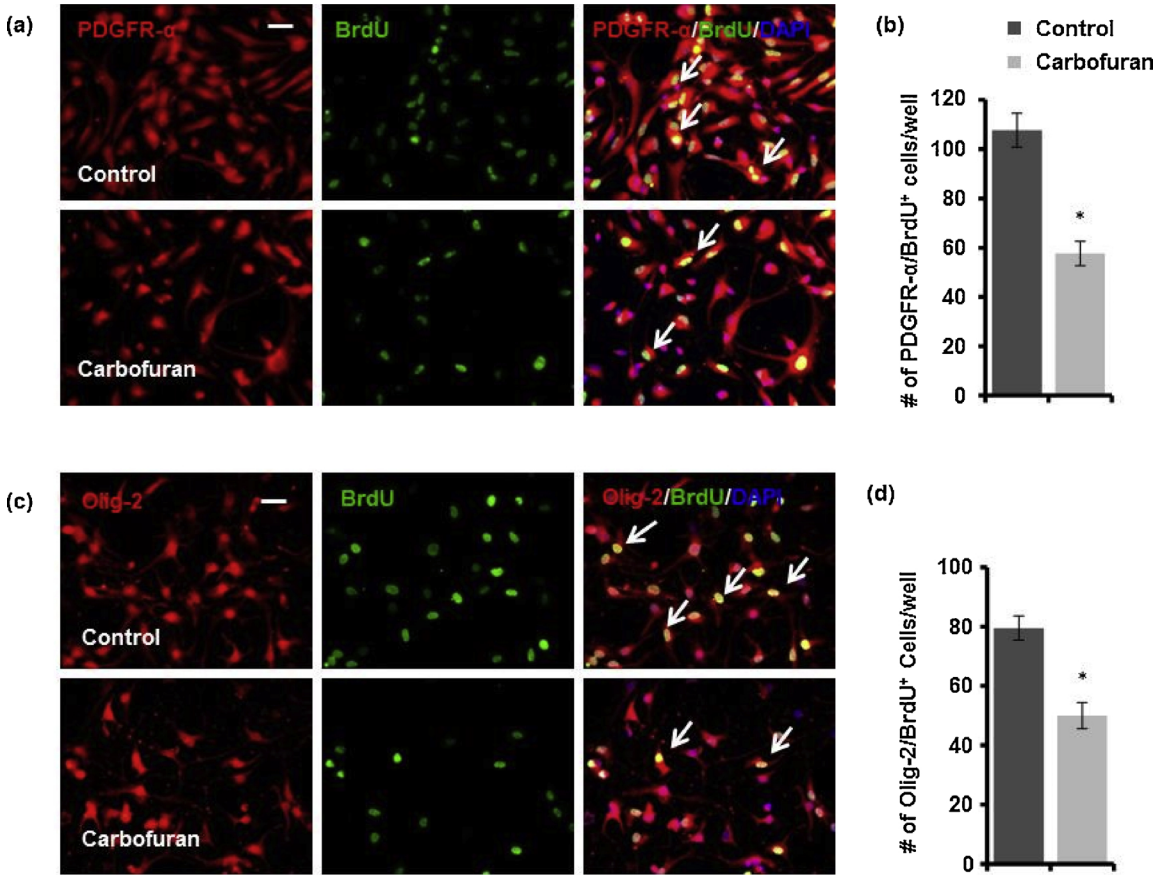

Fig. 2. BrdU incorporation assay showing effects of carbofuran on the proliferation of OPCs in vitro. (a–b) Representative micrographs showing incorporation of BrdU (green) in PDGFR-α^+ cells (red) counterstained with nuclear stain DAPI in OPC culture treated with carbofuran for 24 h. Bar graph from quantitative analysis depicted a significant reduction in number of BrdU/PDGFR-α^+ cells following carbofuran treatment. Arrows indicate co-labeled cells in all the images. (c–d) Representative immunofluorescence images of BrdU/Olig-2 co-labeled cells counterstained with nuclear stain DAPI. Bar diagram showing the number of BrdU/Olig-2 co-labeled cells significantly decreases in the presence of carbofuran as compared to control. Values are expressed as mean ± SEM (n = 3 independent experiments), *p < 0.05 vs control, Scale bar = 20 μm. (For interpretation of the references to colour in this figure legend, the reader is referred to the web version of this article.)

and NF in carbofuran treated rats at both the time points as compared to control (Fig. 8a, b). The data from this study depicted that there were fewer number of myelinated axons in the hippocampus of carbofuran treated rats as compared to control.

3.4. Carbofuran alters the expression of genes and levels of proteins involved in oligodendrocyte development and myelination

We next investigated whether exposure of carbofuran alters the expression of myelination-regulating genes/transcription factors including MBP, CNPase, Olig-2, PDGFR-α, PLP, MAG, myelin oligodendrocyte glycoprotein (MOG), chondroitin sulfate proteoglycan (NG-2), myelin-associated oligodendrocyte basic protein (MOBP) and myelin gene regulatory factor (MRF) in the hippocampus region (Fig. 9a). NG2 glycoprotein is a type I membrane protein expressed in sub-populations of glia including OPCs required for their effective expansion, migration, cell-cycle maintenance and lineage restriction (Karram et al., 2005). We found that carbofuran caused significant down-regulation in the expression of oligodendrocyte lineage-specific genes as such Olig-2, PDGFR-α, NG2 as well as myelination-regulating genes involved in differentiation and maturation of oligodendrocytes such as MBP, CNPase, PLP and MAG in the hippocampus region during both prenatal development and adult stages (Fig. 9a). MRF is a nuclear protein specifically expressed by post-mitotic oligodendrocytes, which acts as a critical transcriptional regulator essential for the expression of other genes such as MBP, MAG, and CNPase (Emery et al., 2009). Carbofuran caused significant down-regulation in the expression of MRF in the hippocampus as compared with control at both the time points studied. However, mRNA expression of MOG and MOBP remained unaltered due to carbofuran exposure at PND21 and PND90 (Fig. 9a).

Further, we examined the effects of carbofuran exposure on the levels of proteins involved in myelination process in the hippocampus. We found that carbofuran significantly decreased the levels of PDGFR-α, MBP, PLP, Olig-2, MAG, and CNPase at both PND21 and PND90 (*p < 0.05) (Fig. 9b–e). Collectively, these results suggested that carbofuran exposure causes a significant decrease in the expression of genes and the levels of proteins involved in oligodendrocyte development which leads to an alteration in their myelination potential in the brain.

3.5. Carbofuran induces apoptosis in oligodendrocytes in the hippocampus of rat brain

Next, we evaluated the effect of carbofuran on the survival of oligodendrocytes in the hippocampus. We analyzed co-localization of cleaved caspase-3, an apoptosis marker with MBP to determine the effect of carbofuran on apoptotic cell death of myelinating oligodendrocytes (Fig. 10). We observed a significant increase in co-localization of cleaved caspase-3 with MBP$^+$ mature oligodendrocytes in the hippocampus of carbofuran treated groups as compared to their respective controls (Fig. 10a, b). To further validate these results, we performed immunoblotting using hippocampal tissue for determining the changes in the levels of important proteins involved in apoptosis. We observed a significant increase in levels of cleaved caspase-3 and pro-apoptotic

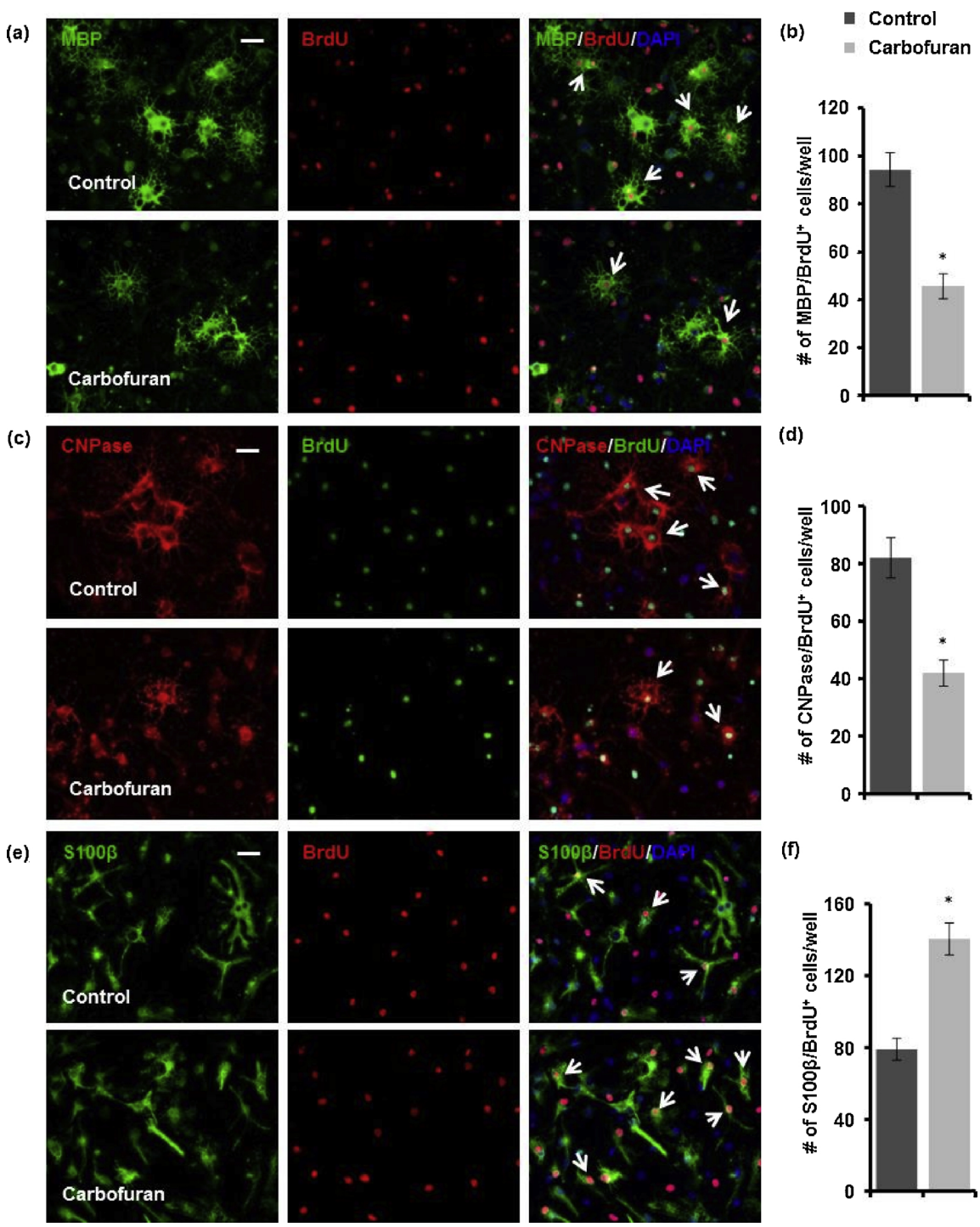

Fig. 3. Carbofuran reduces oligodendrocyte differentiation of OPCs derived from the hippocampus of rat in vitro. Cultured OPCs were subjected to differentiation medium and treated with non-cytotoxic concentration of carbofuran (50 μM). The effects of carbofuran on OPC differentiation and cell fate or commitment were assessed by immunofluorescence co-labeling of BrdU with phenotypic markers of different cell types; (a–b) MBP and (c–d) CNPase for mature oligodendrocyte, and (e–f) S100β for mature astrocytes. Quantitative analysis shows a significant reduction in the number of MBP/BrdU and CNPase/BrdU co-labeled cells and marked increase in the number of S100β/BrdU co-labeled cells following carbofuran treatment as compared to control. Arrows indicate co-labeled cells in all the images.Values are expressed as mean ± SEM (n = 3 independent experiments), *$p < 0.05$ vs control, Scale bar = 20 μm.

protein Bax following carbofuran exposure at both time points (Fig. 10c, d). In contrast, we found significantly decreased levels of anti-apoptotic protein Bcl-2 in the hippocampal tissue of carbofuran exposed groups (Fig. 10c, d). The increase in expression of cleaved caspase-3 in MBP^+ cells suggested that carbofuran induces apoptosis in oligodendrocytes resulting in loss of differentiated and mature myelinating oligodendrocytes in the hippocampus.

3.6. Carbofuran causes ultrastructural changes in myelin sheath in the hippocampus

The effects of carbofuran on myelin architecture in the hippocampus region at the ultrastructural level were observed using TEM. Myelinated axons with compact layers of myelin lamellae were observed in the control animals at both the time periods (Fig. 11a). In

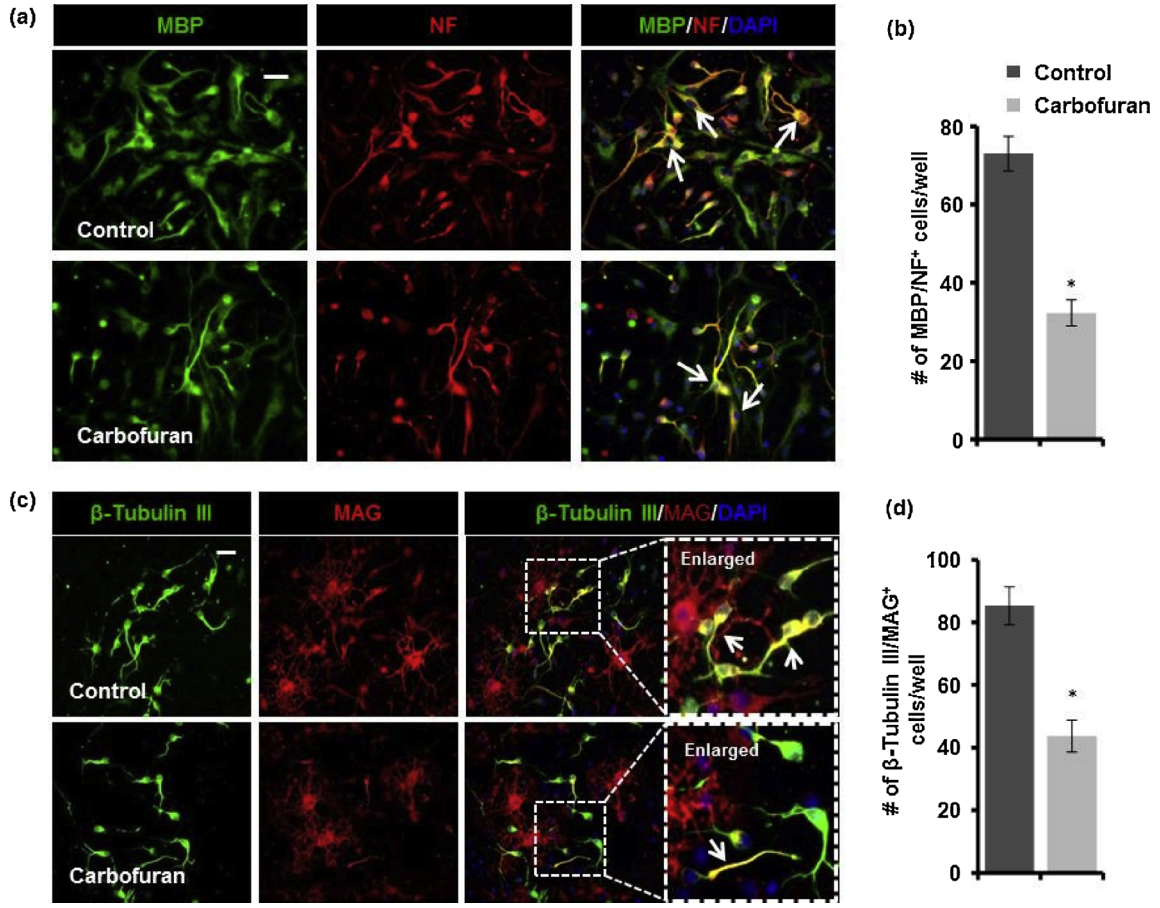

Fig. 4. Effects of carbofuran on myelination potential of oligodendrocytes in vitro. The hippocampal neurons isolated from the rat embryos were seeded in PLL coated chamber slides and allowed to grow for 7 days. The OPCs isolated from the hippocampus of rat embryos were co-cultured with these neurons in the differentiation medium and treated with 50 μM carbofuran. (a–b) Immunofluorescence co-labeling was performed for MBP (green) and NF (red) and counterstained with DAPI (blue). The bar graph shows a significantly reduced number of MBP/NF co-labeled cells following carbofuran treatment in the culture. (c–d) Immunofluorescence co-labeling was performed for β-Tubulin III (green) and MAG (red) and counterstained with DAPI (blue). The bar graph shows a significantly reduced number of myelinated neurons as depicted from the decrease in MAG/β–Tubulin III co-labeled cells following carbofuran treatment in the culture. The enlarged image represents a magnified view of inset within the merged image. Arrows indicate co-labeled cells in all the images. Values are expressed as mean ± SEM (n = 3 independent experiments). *$p < 0.05$ vs control. Scale bar = 20 μm. (For interpretation of the references to colour in this figure legend, the reader is referred to the web version of this article.)

contrast, we found an extensive loosening and disruption of the myelin sheath surrounding the axons in carbofuran treated animals (Fig. 11a). Further, we assessed myelin thickness in context of g-ratio in the myelinated axons present in the hippocampus. The myelin g-ratio is defined as the ratio of the inner to the outer diameter of the myelin sheath. The g-ratio is a fundamental microstructural property of myelinated axons that is widely used as a functional and structural index of optimal axonal myelination. Alteration in the value of g-ratio on either side of its theoretical optimal value of 0.77 causes reduced conduction velocity in the CNS (Chomiak and Hu, 2009). We found that carbofuran exposure causes a significant deviation in g-ratio on both sides of its theoretical optimal value (0.77) among myelinated axons of the hippocampus as compared to control at both the time periods (Fig. 11b). The g-ratio in most of the myelinated axons in carbofuran exposed groups was in the range of 0.50–0.59 reflecting decompaction and loosening of myelin lamellae in the carbofuran exposed groups as compared to control. While a considerably increased number of axons showed the value of g-ratio within a range of 0.80–0.89 which reflects a significant demyelination in axons present in the hippocampus. In contrast, the majority of myelinated axons in control groups showed g-ratio within a range of 0.70–0.79, close to its theoretical optimal value in the CNS. Moreover, we also observed that the number of axons with decompacted myelin was significantly increased due to carbofuran exposure at both time periods (*$p < 0.05$) (Fig. 11c). These results suggested that carbofuran exposure causes significant alteration in myelin architecture surrounding the axons in the hippocampus of rat brain (Additional TEM images for detailed analysis are provided in Supplementary Fig. S2).

3.7. Carbofuran inhibits hippocampus-dependent learning and memory functions

To explore the effects of carbofuran on learning and memory functions in the rats, we performed two-way conditioned avoidance test as a neurobehavioral assay in adult groups (PND90). We noticed a significant decline in learning and memory abilities in terms of decreased CAR by 59.1% and 48.3% respectively in carbofuran exposed animals as compared with control group (*$p < 0.05$, Fig. 12). These results suggested that carbofuran causes cognitive deficits due to defective myelination and impaired oligodendrogenesis in the hippocampus of rat brain.

4. Discussion

Several studies divulged the neurotoxicity of carbofuran and its potential to cause cognitive and behavioral alterations in both animals

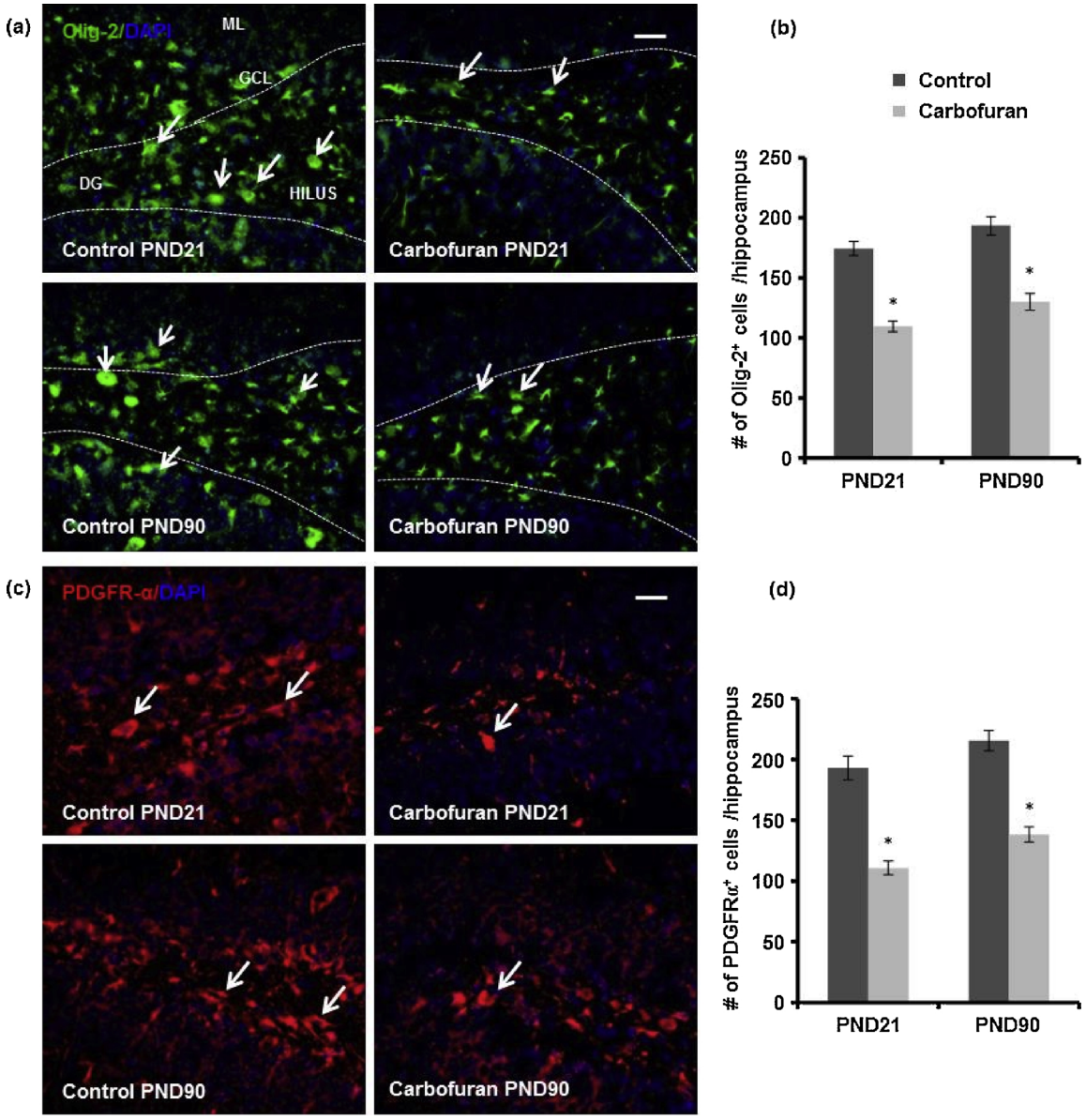

Fig. 5. Carbofuran reduces OPC pool in the hippocampus of rat brain. Immunohistochemical analysis was performed to evaluate the effects of carbofuran on Olig-2 and PDGFR-α immunoreactivity in the hippocampus of the rat brain at PND21 and PND90. (a,b) Immunofluorescence photomicrographs of coronal sections of hippocampus labeled with oligodendrocyte lineage marker Olig-2. Quantitative analysis shows that carbofuran reduces the number of Olig-2$^+$ cells in the hippocampus at both the time points. Arrows indicate Olig-2 immuno-positive cells. ML = molecular layer, DG = dentate gyrus, GCL = granular cell layer. (c,d) Immunofluorescence photomicrographs of hippocampal sections labeled with OPC marker PDGFR-α. Bar diagram showing a reduced number of PDGFR-α$^+$ cells in the hippocampus region following carbofuran exposure as compared to control at both the time points. Arrows indicate PDGFR-α immuno-positive cells. Values are represented as mean ± SEM, n = 6 rat/group, *p < 0.05 vs control. Scale bar = 20 μm.

and humans (Kamboj et al., 2006b; Kamboj and Sandhir, 2007; Seth et al., 2017). Carbofuran causes endocrine disruption, neurobehavioral alternations and reproductive abnormalities when exposed during the gestational as well as postnatal adult period (Goad et al., 2004; Baligar and Kaliwal, 2002). In our previous studies, we demonstrated that gestational carbofuran exposure causes defects in learning and memory abilities of rat offsprings due to inhibition of hippocampal neurogenesis *via* modulation of neurogenic niche asserting the neurotoxic potential of carbofuran and associated behavioral changes (Seth et al., 2017; Mishra et al., 2012). However, the effects of carbofuran on myelination in the hippocampus region of the brain are still unrevealed.

Oligodendrocytes are the chief myelinating cells of the CNS which plays a critical role in shaping neuronal functions in the brain (Saab and Nave, 2017). Myelination insulates the axonal membrane and helps in rapid propagation of nerve impulses (Klingseisen and Lyons, 2018). The event of myelination in most of the mammals starts during late embryonic and early postnatal life, which continues for several years in adults after birth (Young et al., 2013). The principal component of the myelin sheath is myelin lipids and alternations in the levels of total phospholipid, lecithin, sphingomyelin, cholesterol and cerebroside have been speculated in case of many demyelinating diseases (Narayan and Thomas, 2011; Podbielska et al., 2011). The lipid peroxidation also appears to be a major contributing event in the demyelination, possibly through an increase of ROS generation in the brain. It has been reported that carbofuran causes a decline in total phospho-lipid and its fractions in the brain (Gupta et al., 1986). Decreased levels of total phospholipid and increased lipid peroxidation in the brain due to carbofuran exposure might account for constitutional and structural changes in the myelin sheath. Earlier studies have shown that functional acetylcholine receptors (AChR) are present on purified myelin fractions, OPCs and

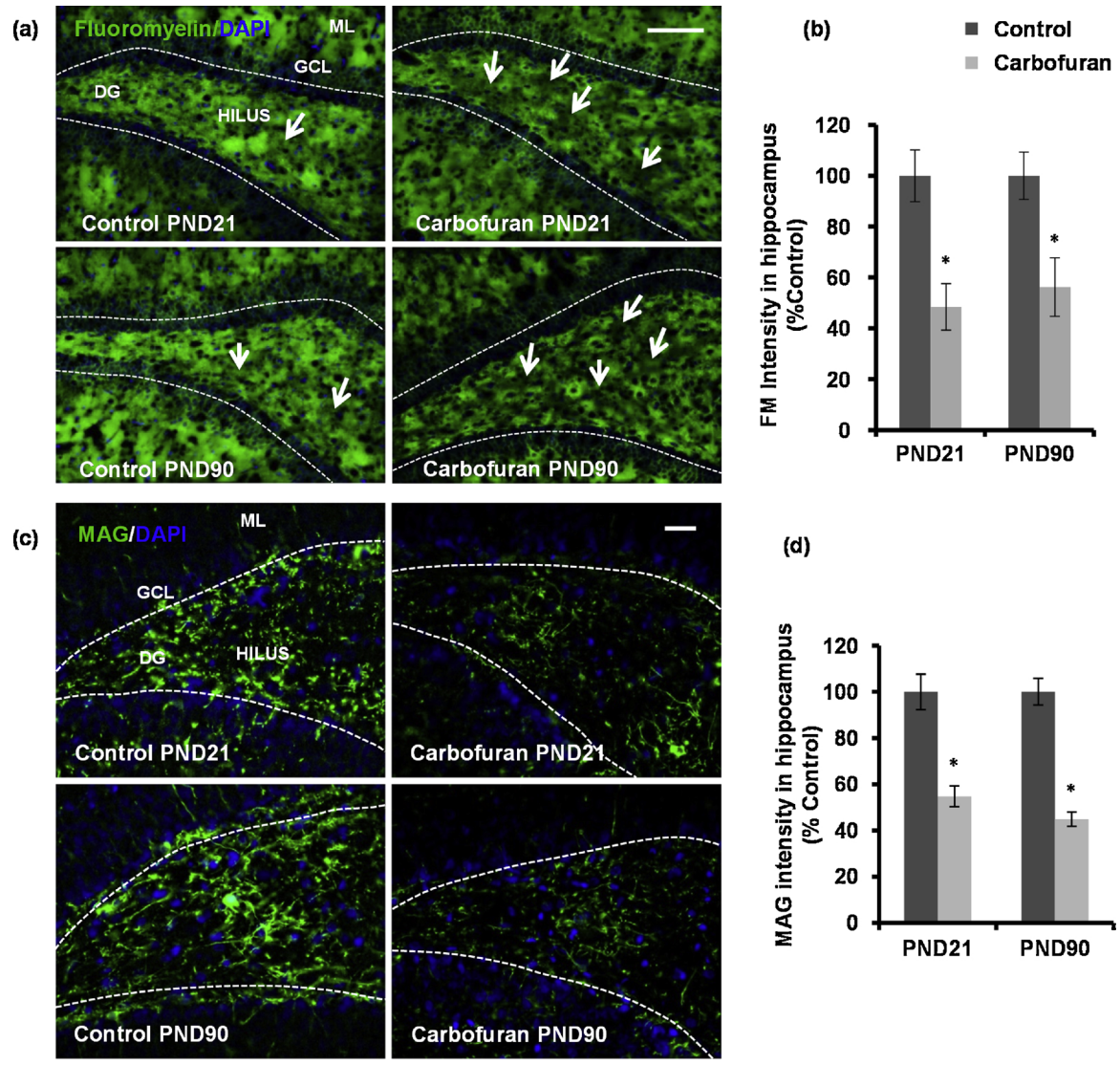

Fig. 6. Carbofuran decreases intensity of fluoromyelin (FM) staining and MAG immunoreactivity in the hippocampus of rat brain. (a–b) Representative images of FM staining (green) counterstained with DAPI (blue) in the DG regions of the hippocampus. Scale bar = 100 μm. Bar diagram suggests that FM intensity was significantly reduced in the hippocampus both at PND21 and PND90 as compared to control. Arrows indicate demyelinated areas in the hippocampus. Scale bar = 100 μm. (c–d) Representative images of hippocampal sections immunostained with MAG (green) counterstained with DAPI (blue). Graphical representation revealed reduced MAG immunoreactivity in the hippocampus region of carbofuran exposed rats at PND21 and PND90. DG = dentate gyrus, ML = molecular layer, GCL = granule cell layer. Values are represented as mean ± SEM, n = 6 rat/group, *p < 0.05 vs control. Scale bar = 20 μm. (For interpretation of the references to colour in this figure legend, the reader is referred to the web version of this article.)

mature oligodendrocyte isolated from the brain (De Angelis et al., 2012; Larocca and Almazan, 1997; Larocca et al., 1987). Although the function of cholinesterase activity in white matter is still not well understood, an earlier study showed that AChE activity peaked during periods of myelination, suggested acetylcholine signaling as a mechanism for functional activity in the axon to stimulate myelination (Kim et al., 1972). Some other studies recognized AChR induced activation of intracellular signaling pathways in OPCs and verified the presence of functional AChR in myelinating glia (Larocca and Almazan, 1997; Takeda et al., 1995). The expression of ACh receptors reported in oligodendrocytes suggests that these cells could be a target for ACh actions and AChE inhibitors. The proliferation, differentiation and survival of OPCs are influenced by activation of AChR in a complex manner that depends on the developmental stage and receptor subtype (Belachew et al., 1998; He and McCarthy, 1994). In the current study, the primary mode of neurotoxicity of carbofuran is the inhibition of AChE, which could also disturb proliferation and differentiation of oligodendrocytes *via* altered ACh signaling.

On the basis of these studies exhibiting the effects of carbofuran on lipid levels and neurobehavioural alterations in rats, we hypothesized that exposure of carbofuran might cause an alteration in the process of myelination. The impaired myelination of hippocampal neurons adversely affects the learning and memory abilities of the organism (Huang et al., 2009). The impairment of axonal myelination in the brain leads to serious consequences including neurological disorders such as schizophrenia and multiple sclerosis (Chambers and Perrone-Bizzozero, 2004; Dulamea, 2017). Therefore, we first performed in vitro studies using hippocampal derived OPCs to determine the effects of carbofuran on their proliferation and differentiation. We observed a concentration-dependent decrease in cell viability of OPCs due to carbofuran similar to those its effects on NSCs (Seth et al., 2017). In line with this, we also found a significant decrease in the incorporation of BrdU in PDGFRα$^+$ and Olig-2$^+$ progenitor cells of oligodendrocytes, suggesting that carbofuran hampers proliferation of OPCs in the culture conditions. Further, we observed that treatment of carbofuran remarkably decreased differentiation of OPCs into mature oligodendrocytes as observed by a

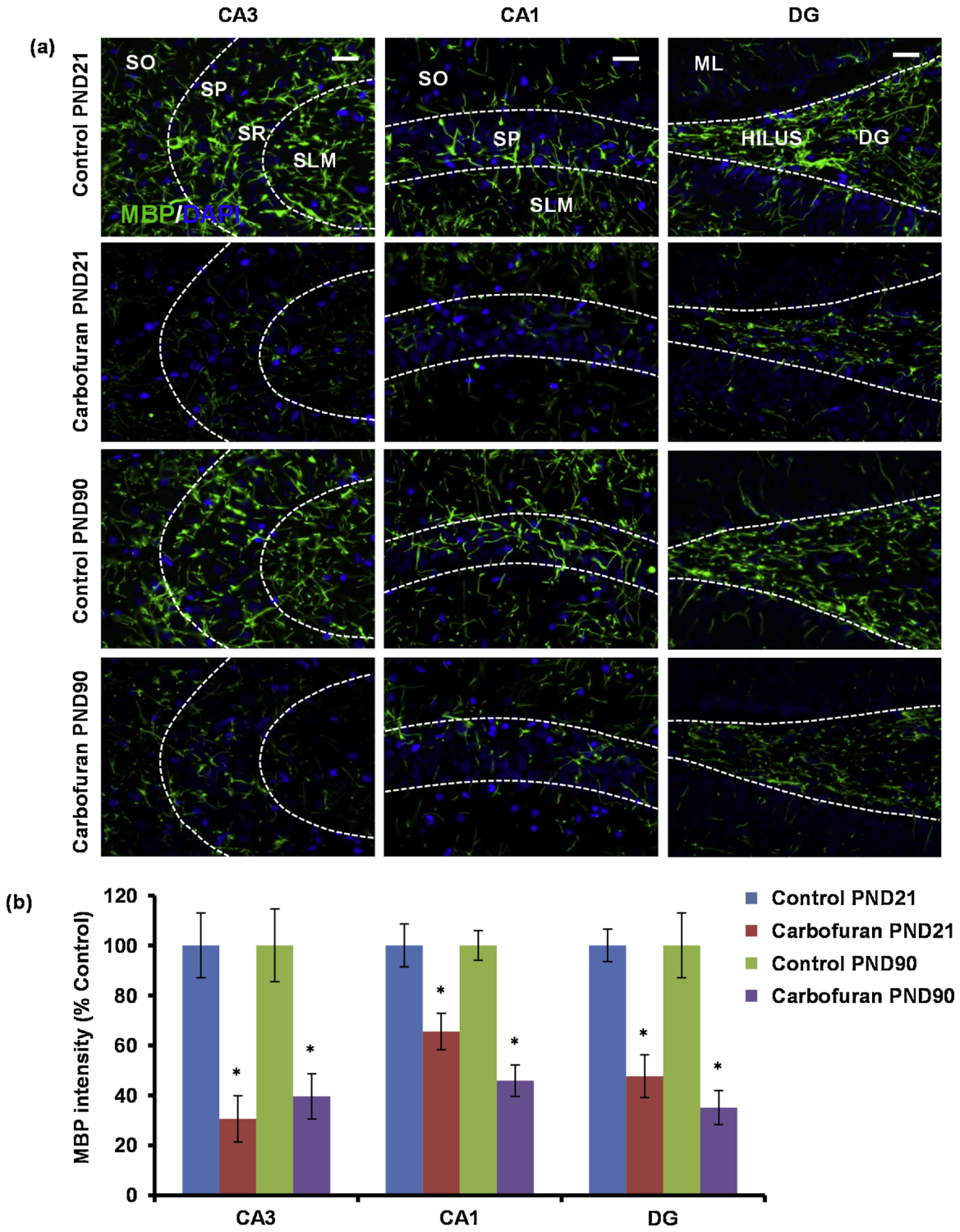

Fig. 7. Carbofuran reduces immunoreactivity of MBP in early postnatal and adult hippocampus of the rat brain. (a) Representative fluorescence images showing hippocampal sections of the brain immunostained with MBP. The MBP^+ fibers are most abundantly visualized in the hilus region of DG and stratum oriens of CA3. (b) Graphical representation of immunoreactivity of MBP in different regions of the hippocampus at PND21 and PND90. DG = dentate gyrus, CA = cornu ammonis, SLM = stratum lacunosum-moleculare, ML = molecular layer, GCL = granule cell layer, SR = stratum radiatum, SO = stratum oriens. Values represented as mean ± SEM, n = 6 rat/group, *p < 0.05 vs control. Scale bar = 20 μm.

reduction in the number of $MBP/BrdU^+$ and $CNPase/BrdU^+$ cells in vitro. Interestingly, we found that stress imposed by carbofuran treatment diverts OPCs towards astrocyte fate as depicted from the increased number of $S100\beta/BrdU^+$ cells in vitro. These findings are corroborated by an earlier study showing stress conditions like white matter stroke induces astrocytic transformation of OPCs (Sozmen et al., 2016). A recent study showed that elevation in S100β protein levels also leads to induce an inflammatory response and impaired oligodendrogenesis in the brain (Santos et al., 2018).

The process of myelination involves a complex sequence of events including proliferation, migration, differentiation of OPCs and their maturation into myelinating oligodendrocytes (Simons and Nave,

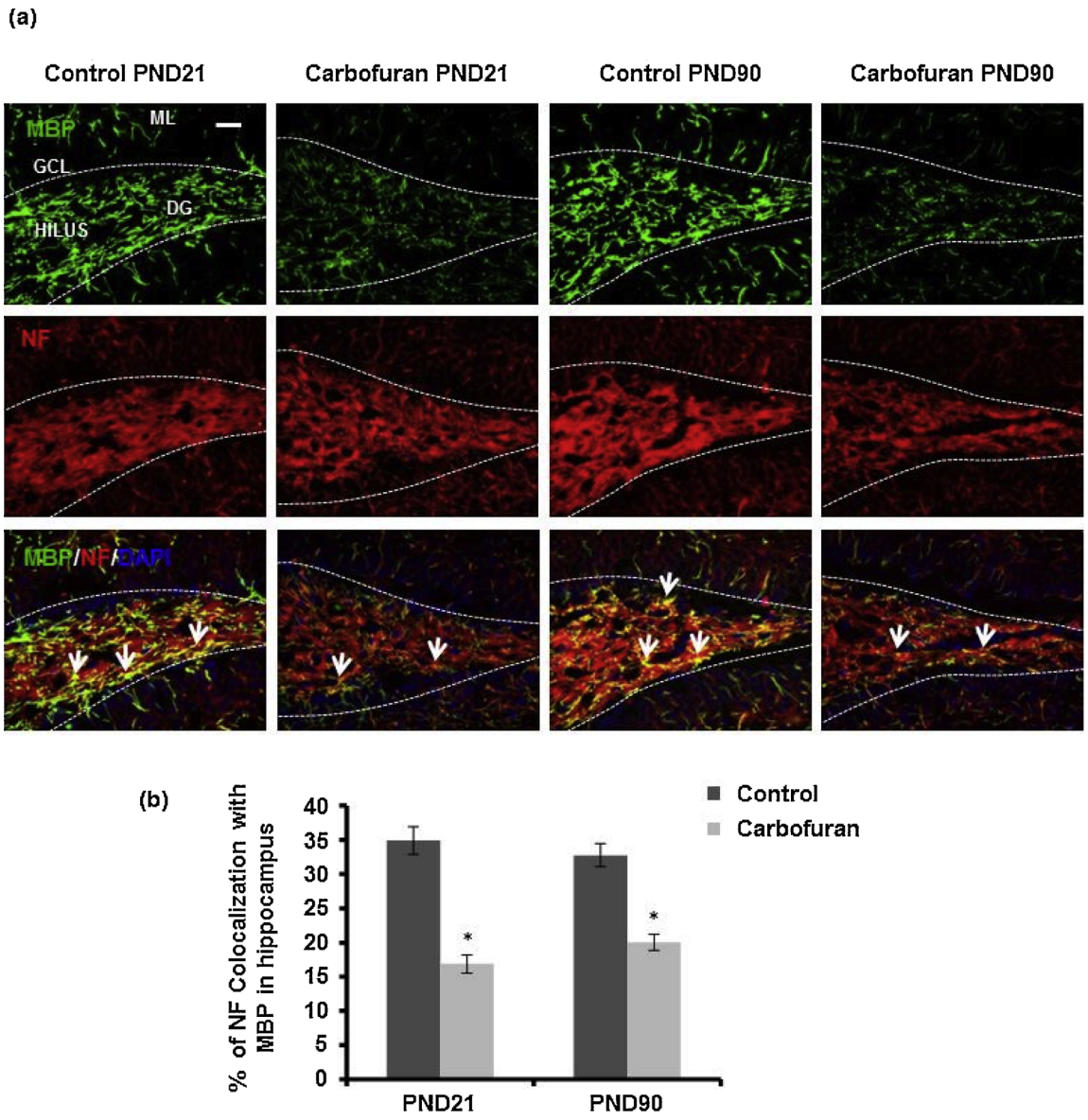

Fig. 8. Effects of carbofuran on immunostaining for MBP and NF in the hippocampus at PND21 and PND90. (a) Representative images showing MBP and NF-positive fibers in DG region of the hippocampus. (b) Quantitative analysis of Manders coefficient showed that the co-localization MBP/NF was significantly reduced in carbofuran treated groups at both the time points. Values represented as mean ± SEM, n = 6 rat/group, *p < 0.05 vs control. Scale bar = 20 μm.

2015). Interference with any of these critical events due to carbofuran exposure could disrupt the normal process of myelin formation in the brain. Therefore, we also investigated the effects of carbofuran on myelination in the hippocampus during prenatal (GD7–PND21) and postnatal (PND21–PND90) brain development by assessing various markers for different stages of oligodendrocyte development.

Olig-2 is a basic helix-loop-helix transcription factor which is associated with specification and differentiation of OPCs (Wang et al., 2014). Ablation of Olig-2 in OPCs has been reported to attenuate differentiation and myelination in the spinal cord (Lu et al., 2002). In the present study, we found that the number of Olig-2^+ progenitors of oligodendrocytes significantly decreased in the hippocampus of carbofuran treated groups as compared to their respective controls at both the time points. A direct negative effect of carbofuran on the pool of OPCs was further indicated by the reduced number of PDGFR-α^+ cells in the hippocampus of carbofuran exposed rats.

Further, immunofluorescence staining showed significantly reduced fluoromyelin intensity and immunoreactivity of MBP and MAG in the hippocampus following carbofuran exposure as compared to the control of matching age. MBP is an essential structural component for the formation of the multilamellar myelin sheath and functions as adhesives for compact myelin formation. Neurofilament proteins (NF) are the major component of cytoskeleton of mature neurons that determine the shape of cells, caliber of axonal projections, and maintenance of axonal transport (Wang et al., 2012). We found carbofuran exposure reduces MBP/NF co-labeling in the hippocampus as well as MAG/β-Tubulin co-labeled cells in vitro, suggesting reduced myelination potential of oligodendrocytes in axons of hippocampal neurons. Progressive loss of myelin also results in axonal degeneration due to the disruption of axon-oligodendrocyte signaling (Alizadeh et al., 2015). Thus, reduced co-localization of MBP/NF due to carbofuran leads to altered axon caliber, which might be a possible reason for cognitive dysfunction. Similarly, other environmental contaminants such as heavy metals also induced demyelination in the CNS (Brubaker et al., 2009; Rai et al., 2013). MAG is a transmembrane glycoprotein that is selectively localized to oligodendroglial membranes (Pronker et al., 2016). Ablation of MAG results in axonal injury with focal swellings and spheroids formation (Loers et al., 2004). Carbofuran exposure also

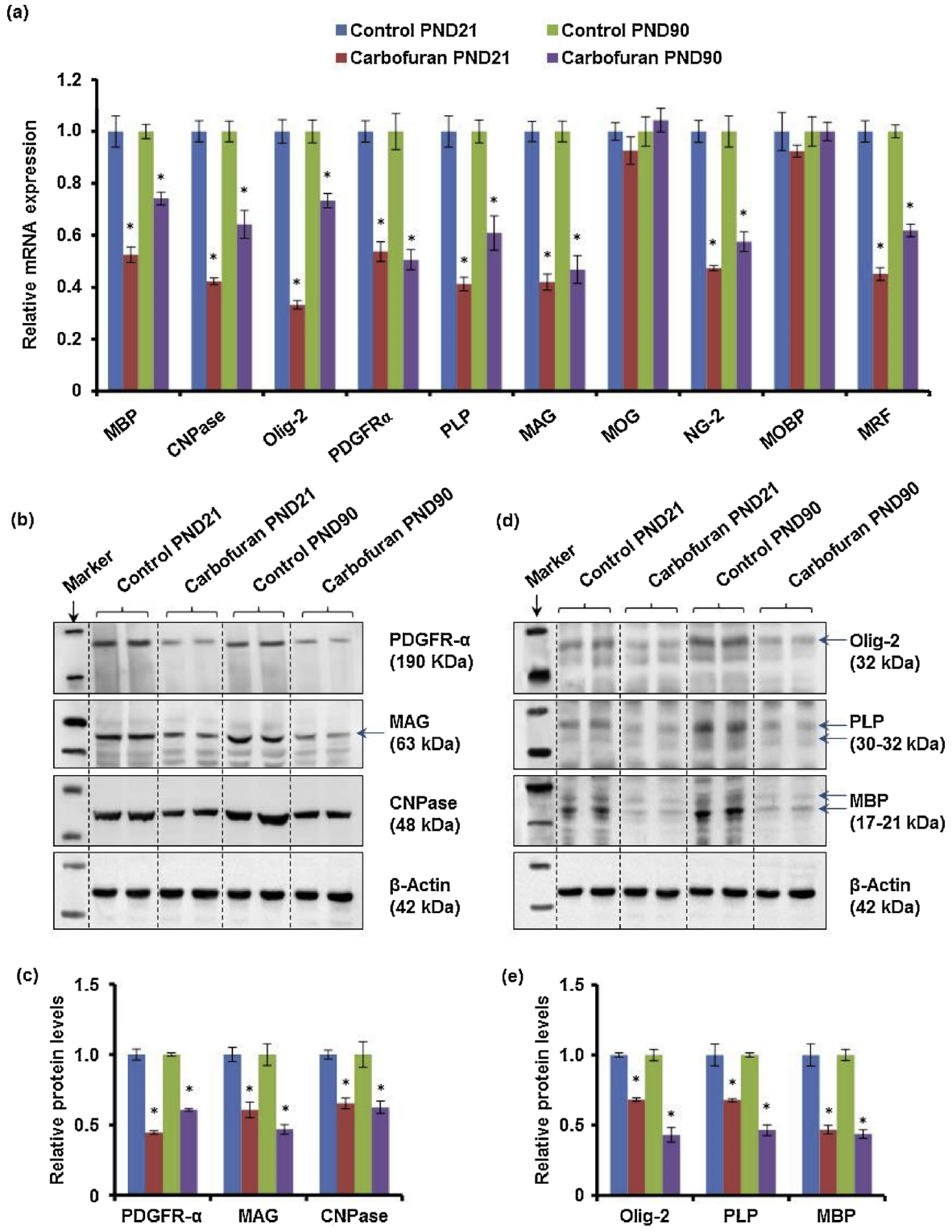

Fig. 9. Carbofuran alters expression of genes and levels of proteins associated with myelination in the hippocampus. (a) Effects of carbofuran on the expression of genes involved in myelination in the hippocampal tissue of the brain at PND21 and PND90 was studied by qRT-PCR. β-actin served as a housekeeping gene for normalization. (b–e) Western blot analysis of the levels of PDGFR-α, MAG, CNPase, Olig-2, PLP and MBP proteins in the hippocampal tissues at PND21 and PND90. The relative protein levels were normalized to β-actin. Values are expressed as mean ± SEM (n = 6 rats/group). *p < 0.05 vs control.

reduced immunoreactivity of MAG in the hippocampus region at both the time points, which may be responsible for disruption of myelin sheath.

The process of myelination and oligodendrocyte maturation is regulated by coordinated expression of several specific genes during the development of brain. We observed down-regulation of Olig-2, NG2 and PDGFR-α genes involved in oligodendrocyte lineage specification due to carbofuran exposure. We also found that carbofuran reduces the expression of MBP, PLP, CNPase, MAG and MRF genes, which are actively involved in oligodendrocyte maturation and functional myelin sheath formation. MRF is a key regulator and direct activator of many genes important in the production of myelin. It has also been reported

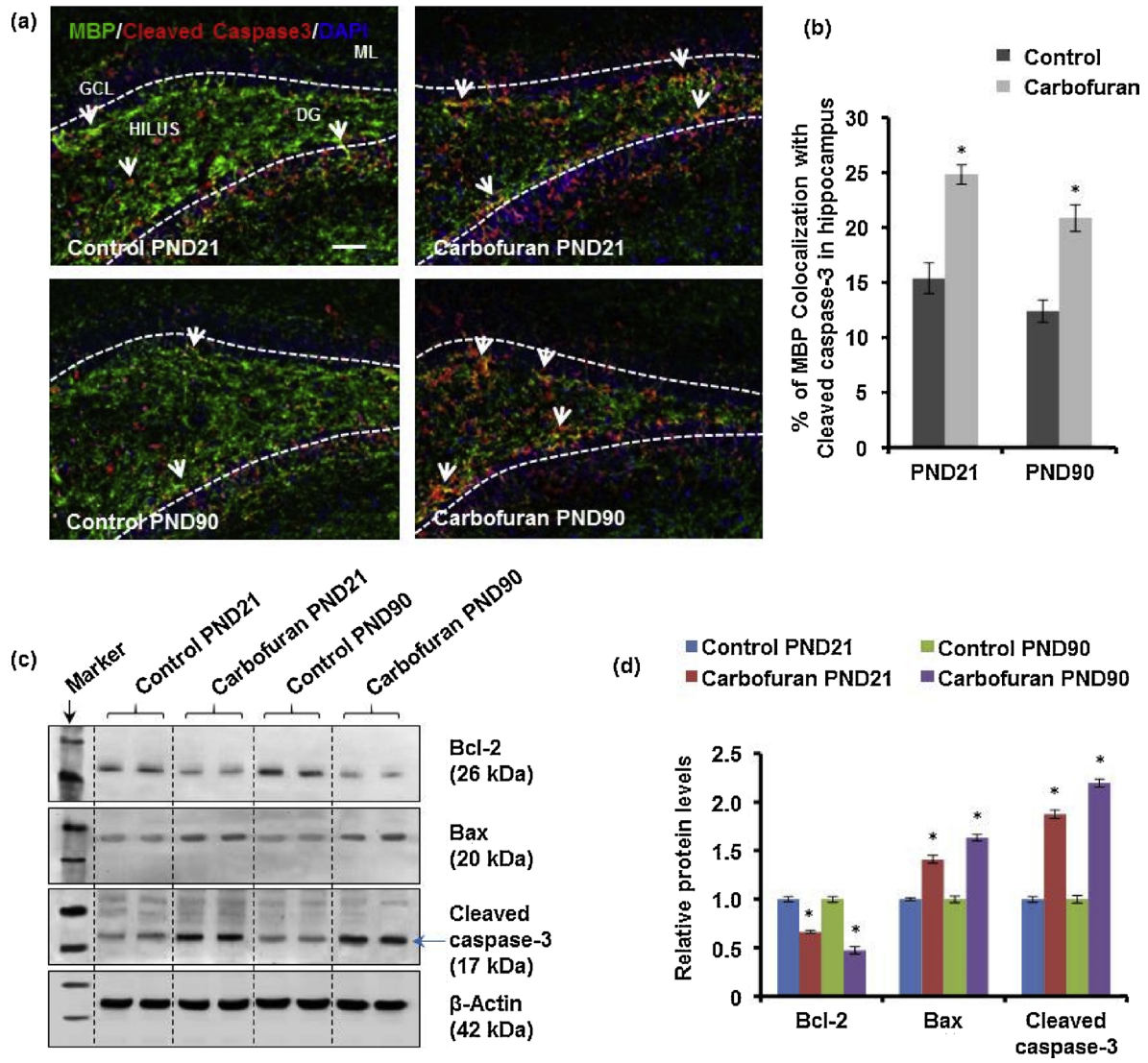

Fig. 10. Carbofuran induces apoptosis of oligodendrocytes in the hippocampus of rat brain. (a–b) Immunofluorescence co-labeling was performed for Cleaved caspase-3 (red) and MBP (green). Bar graph shows co-localization of Cleaved Caspase-3 and MBP significantly increased in the hippocampus of carbofuran treated rats at PND21 and PND90. Values are expressed as mean ± SEM (n = 6 rats per group). Scale bar = 20 μm. *p < 0.05 vs control (c–d) Western blot analysis suggests significantly increased levels of pro-apoptotic protein Bax and cleaved caspase-3 and reduced levels of anti-apoptotic protein Bcl-2 in the hippocampus tissue dissected from carbofuran treated rats. Values are expressed as mean ± SEM (n = 6). *p < 0.05 vs control. (For interpretation of the references to colour in this figure legend, the reader is referred to the web version of this article.)

that genes important in the development and maintenance of myelin sheaths such MAG, PLP, MBP and MOG were down-regulated following ablation of MRF (Emery et al., 2009). Therefore, low expression of MRF due to carbofuran exposure might be one of the major responsible factors for reduced myelination in the hippocampus of brain. These findings were further substantiated by results obtained from immunoblotting of proteins involved in myelination and oligodendrocyte development. The low levels of PDGFR-α and Olig-2 proteins in carbofuran treated rats confer anti-proliferative effects of carbofuran on oligodendrocyte progenitors. While, reduced protein levels of MBP, PLP, CNPase and MAG in carbofuran exposed groups further showed negative effects of this pesticide on oligodendrocyte maturation and axonal myelination. PLP is one of the most abundant proteins in the CNS and has an important role in stabilization of myelin sheath (Lee et al., 2010). CNPase is an enzyme plays a key role in trans-membrane protein-protein interactions for stabilization of myelin sheath (Raasakka and Kursula, 2014). These results suggest that carbofuran causes hypo-myelination in the hippocampus due to noticeable alteration in the expression of genes and proteins involved in the regulation of OPCs proliferation and oligodendrocyte maturation.

Next, we checked the ultrastructural changes in myelin sheath using electron microscopy post carbofuran exposure at both the time periods. It is generally believed that the myelinated axons constrain themselves to achieve maximal efficiency and conduction velocity with a balanced set-point of g-ratio in the CNS (Chomiak and Hu, 2009). We observed a deviation of g-ratio from its theoretical optimum value (~0.77) in carbofuran treated rats. Most of the myelinated axons showed lower values of g-ratio reflecting significant de-compaction and loosening of the multi-laminated sheath in carbofuran exposed rats. Many of the axons exhibited higher g-ratio values than an optimum set point in the carbofuran exposed groups representing significant demyelination in the hippocampus. The adhesion molecules such as hydrophobic PLP, MBP and MAG execute a crucial role in the formation and maintenance of compact myelin sheath (Baumann and Pham-Dinh, 2001). As we observed decreased levels of these proteins in carbofuran treated rats, it could be one of the possible reasons for the increased decompaction of myelin following carbofuran exposure.

Several reports have been documented the role of carbofuran in the

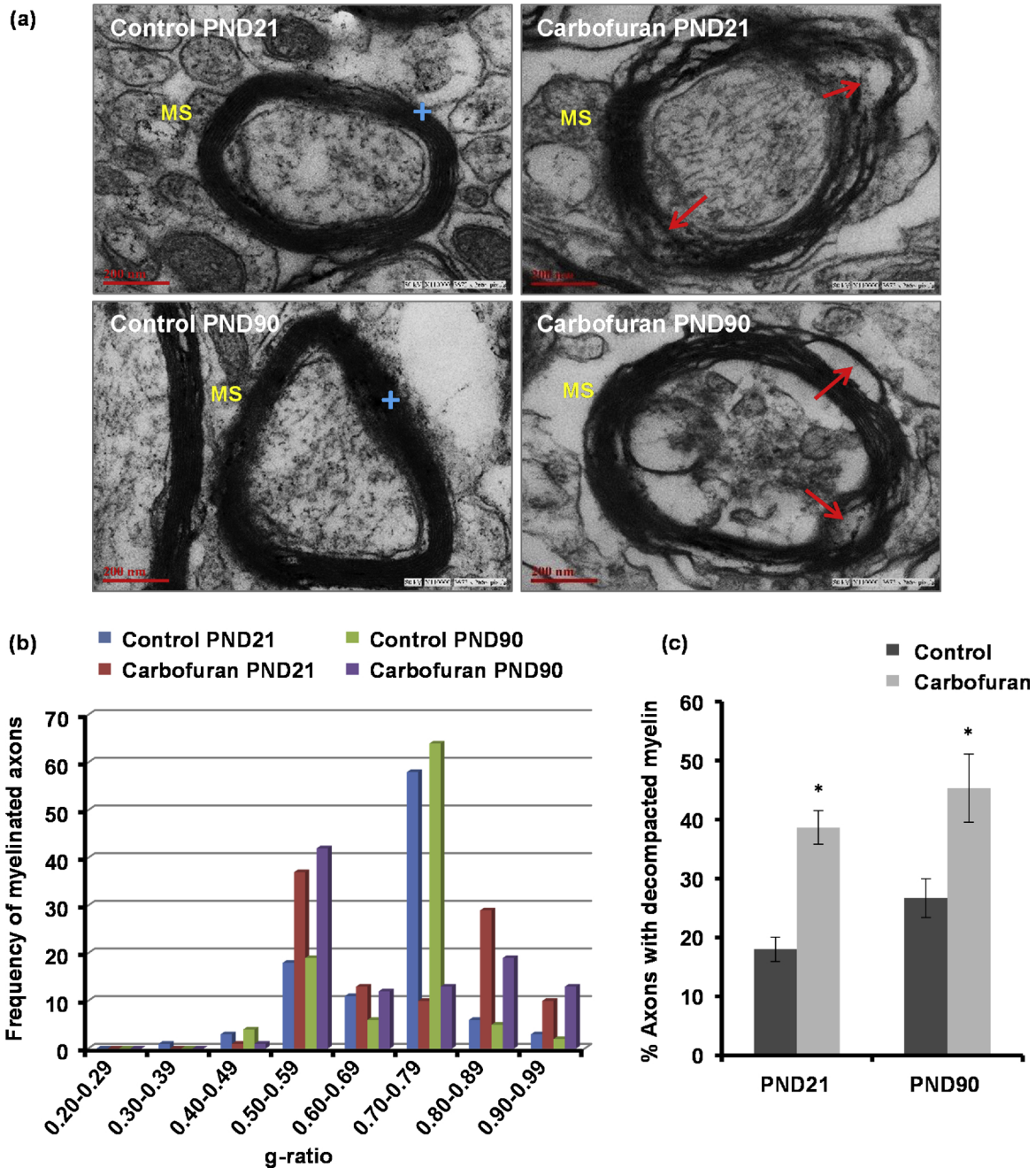

Fig. 11. Carbofuran disturbs myelin architecture in the hippocampus of rat brain. (a) Representative electron microscopic images showing ultrastructure of myelinated axons of control and carbofuran exposed group at PND21 and PND90. Plus sign indicates normal compacted myelinated axons and arrows indicate axons with a decompacted myelin sheath. Scale bar = 200 nm. (b) Bar graph showing alteration in g-ratio among myelinated axons following carbofuran exposure in PND21 and PND90 groups. (c) Bar graph suggesting an increase in the number of axons with decompacted myelin sheath in carbofuran exposed group at both time points. Data are expressed as mean ± SEM (n = 6 rats/group). *p < 0.05 vs control.

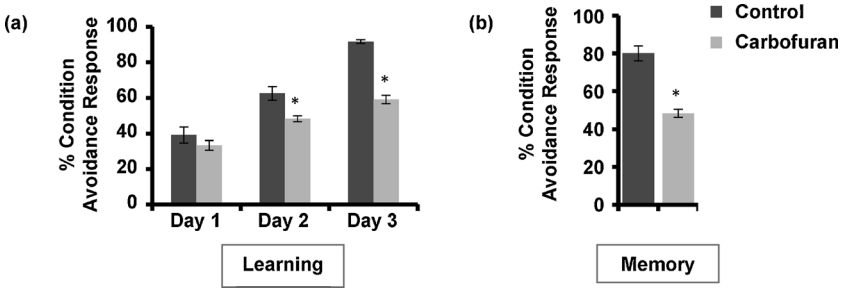

Fig. 12. Carbofuran alters learning and memory abilities of rats. (a–b) The learning and memory was measured following assessment of two- way conditioned avoidance behavior using shuttle-box apparatus in rats of PND90 group. Carbofuran exposed rats showed poor learning and memory performance as compared to control rats. Data were represented as mean ± SEM, n = 6 rats/group, *p < 0.05 vs control.

generation of oxidative stress and apoptosis in the brain (Gupta et al., 2007; Jaiswal et al., 2014). In the present study, we also found that carbofuran induces apoptosis in mature oligodendrocytes as suggested by increased MBP/Cleaved caspase-3 co-localization and altered key determinants of apoptosis (Bax and Bcl2 protein levels) in the hippocampus resulting in the reduced survival of oligodendrocytes. Several pieces of evidence suggest the involvement of myelin in cognition, development of skills, learning and memory (Chambers and Perrone-Bizzozero, 2004; Chao et al., 2018; Wischhof et al., 2015). Therefore, we studied the effects of carbofuran exposure on cognitive function of the rats. We observed that carbofuran treated rats showed poor learning and memory performance in active avoidance test. Therefore, learning and memory deficits in carbofuran treated rats can be correlated with significant loss of myelin and OPCs pool in the hippocampus. These findings are corroborated by previous studies which showed altered cognitive abilities in rats following carbofuran exposure (Kamboj and Sandhir, 2007; Seth et al., 2017; Kamboj et al., 2006b). During gestation, the liver and blood-brain barrier in the fetus are poorly developed due to which they are not able to detoxify carbofuran and it easily approaches to brain tissue. So, even small amount of carbofuran exposure during the short period of prenatal development causes extensive damage and exhibits almost similar neurotoxic effects in comparison to its exposure for longer duration in adults. Thus, we observed almost similar effects of carbofuran on myelination during its prenatal and adult exposure. Further work is required to dissect the exact molecular mechanism underlying demyelination caused by carbofuran exposure. Carbofuran may affect myelination through a variety of mechanisms beyond its property of cholinesterase inhibition. Notch and TGF-β signaling pathways are known to regulate OPC proliferation and differentiation (Zhang et al., 2009; Palazuelos et al., 2014). The upregulation of TGF-β signaling in OPCs causes reduced proliferation (Palazuelos et al., 2014). In our previous study, we have found that carbofuran increases TGF-β levels and its downstream regulators in the hippocampus resulting in inhibition of hippocampal neurogenesis, which could be another explanation for the possible mechanism underlying carbofuran mediated altered myelination (Seth et al., 2017).

Altogether, these results suggest that carbofuran significantly inhibits myelination potential in the hippocampus due to impaired proliferation, maturation and survival of oligodendrocytes.

5. Conclusions

Conclusively, our study demonstrated that prenatal and post-natal carbofuran exposure inhibits proliferation, maturation and differentiation of OPC, and induces apoptosis in oligodendrocytes resulting impaired myelination in the hippocampus region of rat brain. The impaired myelination due to carbofuran was found to be associated with learning and memory defects in the rats. In future, further elucidation of the cellular and molecular mechanisms of carbofuran mediated impaired myelination is required to better understand the impact of this pesticide exposure during critical periods of the brain development.

Conflict of interest

The authors declare no competing financial interests.

Acknowledgments

This work was supported by the Lady Tata Memorial-U.K. Young Scientist Grant, Science and Engineering Research Board (SERB)-New Delhi, EMR grant (EMR/2016/001933) and Department of Biotechnology, New Delhi research grant (BT/PR15819/MED/31/322/2015) to RKC. We are thankful to the Director, CSIR-IITR for constant support during this study. BS and AY are recipients of Senior Research Fellowship from CSIR and UGC, New Delhi respectively. CSIR-IITR Manuscript Communication number-3540.

References

Agarwal, S., Tiwari, S.K., Seth, B., Yadav, A., Singh, A., Mudawal, A., Chauhan, L.K., Gupta, S.K., Choubey, V., Tripathi, A., Kumar, A., Ray, R.S., Shukla, S., Parmar, D., Chaturvedi, R.K., 2015. Activation of Autophagic flux against xenoestrogen bisphenol-A-induced hippocampal neurodegeneration via AMP kinase (AMPK)/mammalian target of rapamycin (mTOR) pathways. J. Biol. Chem. 290 (34), 21163–21184. https://doi.org/10.1074/jbc.M115.648998.

Agarwal, S., Yadav, A., Tiwari, S.K., Seth, B., Chauhan, L.K., Khare, P., Ray, R.S., Chaturvedi, R.K., 2016. Dynamin-related protein 1 inhibition mitigates bisphenol a-mediated alterations in mitochondrial dynamics and neural stem cell proliferation and differentiation. J. Biol. Chem. 291 (31), 15923–15939. https://doi.org/10.1074/jbc.M115.709493.

Agnish, N.D., Keller, K.A., 1997. The rationale for culling of rodent litters. Fundam. Appl. Toxicol. 38 (1), 2–6.

Alizadeh, A., Dyck, S.M., Karimi-Abdolrezaee, S., 2015. Myelin damage and repair in pathologic CNS: challenges and prospects. Front. Mol. Neurosci. 8, 35. https://doi.org/10.3389/fnmol.2015.00035.

Baligar, P.N., Kaliwal, B.B., 2002. Reproductive toxicity of carbofuran to the female mice: effects on estrous cycle and follicles. Ind. Health 40 (4), 345–352.

Baumann, N., Pham-Dinh, D., 2001. Biology of oligodendrocyte and myelin in the mammalian central nervous system. Physiol. Rev. 81 (2), 871–927. https://doi.org/10.1152/physrev.2001.81.2.871.

Belachew, S., Malgrange, B., Rigo, J.M., Rogister, B., Coucke, P., Mazy-Servais, C., Moonen, G., 1998. Developmental regulation of neuroligand-induced responses in cultured oligodendroglia. Neuroreport 9 (6), 973–980.

Brewer, G.J., Torricelli, J.R., 2007. Isolation and culture of adult neurons and neurospheres. Nat. Protoc. 2 (6), 1490–1498. https://doi.org/10.1038/nprot.2007.207.

Brubaker, C.J., Schmithorst, V.J., Haynes, E.N., Dietrich, K.N., Egelhoff, J.C., Lindquist, D.M., Lanphear, B.P., Cecil, K.M., 2009. Altered myelination and axonal integrity in adults with childhood lead exposure: a diffusion tensor imaging study. Neurotoxicology 30 (6), 867–875. https://doi.org/10.1016/j.neuro.2009.07.007.

Chahal, K.S., Prakash, A., Majeed, A.B., 2015. The role of multifunctional drug therapy against carbamate induced neuronal toxicity during acute and chronic phase in rats. Environ. Toxicol. Pharmacol. 40 (1), 220–229. https://doi.org/10.1016/j.etap.2015.06.002.

Chambers, J.S., Perrone-Bizzozero, N.I., 2004. Altered myelination of the hippocampal formation in subjects with schizophrenia and bipolar disorder. Neurochem. Res. 29 (12), 2293–2302.

Chao, F.L., Zhang, L., Zhang, Y., Zhou, C.N., Jiang, L., Xiao, Q., Luo, Y.M., Lv, F.L., He, Q., Tang, Y., 2018. Running exercise protects against myelin breakdown in the absence of neurogenesis in the hippocampus of AD mice. Brain Res. https://doi.org/10.1016/j.brainres.2018.01.007.

Chen, N.N., Luo, D.J., Yao, X.Q., Yu, C., Wang, Y., Wang, Q., Wang, J.Z., Liu, G.P., 2012. Pesticides induce spatial memory deficits with synaptic impairments and an imbalanced tau phosphorylation in rats. J. Alzheimers Dis. 30 (3), 585–594. https://doi.org/10.3233/JAD-2012-111946.

Chomiak, T., Hu, B., 2009. What is the optimal value of the g-ratio for myelinated fibers in the rat CNS? A theoretical approach. PLoS One 4 (11), e7754. https://doi.org/10.1371/journal.pone.0007754.

De Angelis, F., Bernardo, A., Magnaghi, V., Minghetti, L., Tata, A.M., 2012. Muscarinic receptor subtypes as potential targets to modulate oligodendrocyte progenitor survival, proliferation, and differentiation. Dev. Neurobiol. 72 (5), 713–728. https://doi.org/10.1002/dneu.20976.

de Castro, F., Bribian, A., 2005. The molecular orchestra of the migration of oligodendrocyte precursors during development. Brain Res. Brain Res. Rev. 49 (2), 227–241. https://doi.org/10.1016/j.brainresrev.2004.12.034.

Doretto, S., Malerba, M., Ramos, M., Ikrar, T., Kinoshita, C., De Mei, C., Tirotta, E., Xu, X., Borrelli, E., 2011. Oligodendrocytes as regulators of neuronal networks during early postnatal development. PLoS One 6 (5), e19849. https://doi.org/10.1371/journal.pone.0019849.

Dulamea, A.O., 2017. Role of oligodendrocyte dysfunction in demyelination, remyelination and neurodegeneration in multiple sclerosis. Adv. Exp. Med. Biol. 958, 91–127. https://doi.org/10.1007/978-3-319-47861-6_7.

Dutta, R., Chang, A., Doud, M.K., Kidd, G.J., Ribaudo, M.V., Young, E.A., Fox, R.J., Staugaitis, S.M., Trapp, B.D., 2011. Demyelination causes synaptic alterations in hippocampi from multiple sclerosis patients. Ann. Neurol. 69 (3), 445–454. https://doi.org/10.1002/ana.22337.

Emery, B., Agalliu, D., Cahoy, J.D., Watkins, T.A., Dugas, J.C., Mulinyawe, S.B., Ibrahim, A., Ligon, K.L., Rowitch, D.H., Barres, B.A., 2009. Myelin gene regulatory factor is a critical transcriptional regulator required for CNS myelination. Cell 138 (1), 172–185. https://doi.org/10.1016/j.cell.2009.04.031.

Fruttiger, M., Karlsson, L., Hall, A.C., Abramsson, A., Calver, A.R., Bostrom, H., Willetts, K., Bertold, C.H., Heath, J.K., Betsholtz, C., Richardson, W.D., 1999. Defective oligodendrocyte development and severe hypomyelination in PDGF-A knockout mice. Development 126 (3), 457–467.

Fu, S.L., Hu, J.G., Li, Y., Wang, Y.X., Jin, J.Q., Xui, X.M., Lu, P.H., 2007. A simplified method for generating oligodendrocyte progenitor cells from neural precursor cells isolated from the E16 rat spinal cord. Acta Neurobiol. Exp. 67 (4), 367–377.

Gammon, D.W., Liu, Z., Becker, J.M., 2012. Carbofuran occupational dermal toxicity, exposure and risk assessment. Pest Manag. Sci. 68 (3), 362–370. https://doi.org/10.1002/ps.2270.

Goad, R.T., Goad, J.T., Atieh, B.H., Gupta, R.C., 2004. Carbofuran-induced endocrine disruption in adult male rats. Toxicol. Mech. Methods 14 (4), 233–239. https://doi.org/10.1080/15376520490434476.

Gupta, R.C., Goad, J.T., Kadel, W.L., 1994. In vivo acute effects of carbofuran on protein, lipid, and lipoproteins in rat liver and serum. J. Toxicol. Environ. Health 42 (4), 451–462. https://doi.org/10.1080/15287399409531895.
Gupta, R.C., Milatovic, S., Dettbarn, W.D., Aschner, M., Milatovic, D., 2007. Neuronal oxidative injury and dendritic damage induced by carbofuran: protection by memantine. Toxicol. Appl. Pharmacol. 219 (2–3), 97–105. https://doi.org/10.1016/j.taap.2006.10.028.
Gupta, M., Mukherjee, S., Gupta, S.D., Dolui, A.K., Dey, S.N., Roy, D.K., 1986. Changes of lipid spectrum in different tissues of Furadan-treated mice. Toxicology 38 (1), 69–79.
He, M., McCarthy, K.D., 1994. Oligodendroglial signal transduction systems are developmentally regulated. J. Neurochem. 63 (2), 501–508.
Huang, Z., Liu, J., Cheung, P.Y., Chen, C., 2009. Long-term cognitive impairment and myelination deficiency in a rat model of perinatal hypoxic-ischemic brain injury. Brain Res. 1301, 100–109. https://doi.org/10.1016/j.brainres.2009.09.006.
Jaiswal, S.K., Siddiqi, N.J., Sharma, B., 2014. Carbofuran induced oxidative stress mediated alterations in Na(+)-K(+)-ATPase activity in rat brain: amelioration by vitamin E. J. Biochem. Mol. Toxicol. 28 (7), 320–327. https://doi.org/10.1002/jbt.21568.
Kamboj, A., Sandhir, R., 2007. Perturbed synaptosomal calcium homeostasis and behavioral deficits following carbofuran exposure: neuroprotection by *N*-acetylcysteine. Neurochem. Res. 32 (3), 507–516. https://doi.org/10.1007/s11064-006-9264-y.
Kamboj, S.S., Kumar, V., Kamboj, A., Sandhir, R., 2008. Mitochondrial oxidative stress and dysfunction in rat brain induced by carbofuran exposure. Cell. Mol. Neurobiol. 28 (7), 961–969. https://doi.org/10.1007/s10571-008-9270-5.
Kamboj, A., Kiran, R., Sandhir, R., 2006a. *N*-Acetylcysteine ameliorates carbofuran-induced alterations in lipid composition and activity of membrane bound enzymes. Mol. Cell. Biochem. 286 (1–2), 107–114. https://doi.org/10.1007/s11010-005-9100-8.
Kamboj, A., Kiran, R., Sandhir, R., 2006b. Carbofuran-induced neurochemical and neurobehavioral alterations in rats: attenuation by *N*-acetylcysteine. Exp. Brain Res. 170 (4), 567–575. https://doi.org/10.1007/s00221-005-0241-5.
Karram, K., Chatterjee, N., Trotter, J., 2005. NG2-expressing cells in the nervous system: role of the proteoglycan in migration and glial-neuron interaction. J. Anat. 207 (6), 735–744. https://doi.org/10.1111/j.1469-7580.2005.00461.x.
Kim, S.U., TH, O., Johnson, D.D., 1972. Developmental changes of acetylcholinesterase and pseudocholinesterase in organotypic cultures of spinal cord. Exp. Neurol. 35 (2), 274–281.
Klingseisen, A., Lyons, D.A., 2018. Axonal regulation of central nervous system myelination: structure and function. Neuroscientist 24 (1), 7–21. https://doi.org/10.1177/1073858417703030.
Larocca, J.N., Almazan, G., 1997. Acetylcholine agonists stimulate mitogen-activated protein kinase in oligodendrocyte progenitors by muscarinic receptors. J. Neurosci. Res. 50 (5), 743–754. https://doi.org/10.1002/(SICI)1097-4547(19971201)50:5<743::AID-JNR11>3.0.CO;2-2.
Larocca, J.N., Ledeen, R.W., Dvorkin, B., Makman, M.H., 1987. Muscarinic receptor binding and muscarinic receptor-mediated inhibition of adenylate cyclase in rat brain myelin. J. Neurosci. 7 (12), 3869–3876.
Lee, D.H., Jeong, J.Y., Kim, Y.S., Kim, J.S., Cho, Y.W., Roh, G.S., Kim, H.J., Kang, S.S., Cho, G.J., Choi, W.S., 2010. Ethanol down regulates the expression of myelin proteolipid protein in the rat hippocampus. Anat. Cell Biol. 43 (3), 194–200. https://doi.org/10.5115/acb.2010.43.3.194.
Li, H., Ricordel, I., Tong, L., Schopfer, L.M., Baud, F., Megarbane, B., Maury, E., Masson, P., Lockridge, O., 2009. Carbofuran poisoning detected by mass spectrometry of butyrylcholinesterase adduct in human serum. J. Appl. Toxicol.: JAT 29 (2), 149–155. https://doi.org/10.1002/jat.1392.
Liu, J., Dietz, K., DeLoyht, J.M., Pedre, X., Kelkar, D., Kaur, J., Vialou, V., Lobo, M.K., Dietz, D.M., Nestler, E.J., Dupree, J., Casaccia, P., 2012. Impaired adult myelination in the prefrontal cortex of socially isolated mice. Nat. Neurosci. 15 (12), 1621–1623. https://doi.org/10.1038/nn.3263.
Loers, G., Aboul-Enein, F., Bartsch, U., Lassmann, H., Schachner, M., 2004. Comparison of myelin, axon, lipid, and immunopathology in the central nervous system of differentially myelin-compromised mutant mice: a morphological and biochemical study. Mol. Cell. Neurosci. 27 (2), 175–189. https://doi.org/10.1016/j.mcn.2004.06.006.
Lu, Q.R., Sun, T., Zhu, Z., Ma, N., Garcia, M., Stiles, C.D., Rowitch, D.H., 2002. Common developmental requirement for Olig function indicates a motor neuron/oligodendrocyte connection. Cell 109 (1), 75–86.
McQueen, J., Reimer, M.M., Holland, P.R., Manso, Y., McLaughlin, M., Fowler, J.H., Horsburgh, K., 2014. Restoration of oligodendrocyte pools in a mouse model of chronic cerebral hypoperfusion. PLoS One 9 (2), e87227. https://doi.org/10.1371/journal.pone.0087227.
Mishra, D., Tiwari, S.K., Agarwal, S., Sharma, V.P., Chaturvedi, R.K., 2012. Prenatal carbofuran exposure inhibits hippocampal neurogenesis and causes learning and memory deficits in offspring. Toxicol. Sci. 127 (1), 84–100. https://doi.org/10.1093/toxsci/kfs004.
Moser, V.C., McDaniel, K.L., Phillips, P.M., Lowit, A.B., 2010. Time-course, dose-response, and age comparative sensitivity of *N*-methyl carbamates in rats. Toxicol. Sci. 114 (1), 113–123. https://doi.org/10.1093/toxsci/kfp286.
Narayan, S., Thomas, E.A., 2011. Sphingolipid abnormalities in psychiatric disorders: a missing link in pathology? Front. Biosci. 16, 1797–1810.
Nickel, M., Gu, C., 2018. Regulation of central nervous system myelination in higher brain functions. Neural Plast. 2018, 6436453. https://doi.org/10.1155/2018/6436453.
Noble, M., 2004. The possible role of myelin destruction as a precipitating event in Alzheimer's disease. Neurobiol. Aging 25 (1), 25–31.
Palazuelos, J., Klingener, M., Aguirre, A., 2014. TGFbeta signaling regulates the timing of CNS myelination by modulating oligodendrocyte progenitor cell cycle exit through SMAD3/4/FoxO1/Sp1. J. Neurosci. 34 (23), 7917–7930. https://doi.org/10.1523/JNEUROSCI.0363-14.2014.
Payne, S.C., Bartlett, C.A., Harvey, A.R., Dunlop, S.A., Fitzgerald, M., 2011. Chronic swelling and abnormal myelination during secondary degeneration after partial injury to a central nervous system tract. J. Neurotrauma 28 (6), 1077–1088. https://doi.org/10.1089/neu.2010.1665.
Pituch, K.C., Moyano, A.L., Lopez-Rosas, A., Marottoli, F.M., Li, G., Hu, C., van Breemen, R., Mansson, J.E., Givogri, M.I., 2015. Dysfunction of platelet-derived growth factor receptor alpha (PDGFRalpha) represses the production of oligodendrocytes from arylsulfatase A-deficient multipotential neural precursor cells. J. Biol. Chem. 290 (11), 7040–7053. https://doi.org/10.1074/jbc.M115.636498.
Podbielska, M., Levery, S.B., Hogan, E.L., 2011. The structural and functional role of myelin fast-migrating cerebrosides: pathological importance in multiple sclerosis. Clin. Lipidol. 6 (2), 159–179. https://doi.org/10.2217/clp.11.8.
Preston, M., Gong, X., Su, W., Matsumoto, S.G., Banine, F., Winkler, C., Foster, S., Xing, R., Struve, J., Dean, J., Baggenstoss, B., Weigel, P.H., Montine, T.J., Back, S.A., Sherman, L.S., 2013. Digestion products of the PH20 hyaluronidase inhibit remyelination. Ann. Neurol. 73 (2), 266–280. https://doi.org/10.1002/ana.23788.
Pronker, M.F., Lemstra, S., Snijder, J., Heck, A.J., Thies-Weesie, D.M., Pasterkamp, R.J., Janssen, B.J., 2016. Structural basis of myelin-associated glycoprotein adhesion and signalling. Nat. Commun. 7, 13584. https://doi.org/10.1038/ncomms13584.
Raasakka, A., Kursula, P., 2014. The myelin membrane-associated enzyme 2',3'-cyclic nucleotide 3'-phosphodiesterase: on a highway to structure and function. Neurosci. Bull. 30 (6), 956–966. https://doi.org/10.1007/s12264-013-1437-5.
Rai, N.K., Ashok, A., Rai, A., Tripathi, S., Nagar, G.K., Mitra, K., Bandyopadhyay, S., 2013. Exposure to As, Cd and Pb-mixture impairs myelin and axon development in rat brain, optic nerve and retina. Toxicol. Appl. Pharmacol. 273 (2), 242–258. https://doi.org/10.1016/j.taap.2013.05.003.
Saab, A.S., Nave, K.A., 2017. Myelin dynamics: protecting and shaping neuronal functions. Curr. Opin. Neurobiol. 47, 104–112. https://doi.org/10.1016/j.conb.2017.09.013.
Santos, G., Barateiro, A., Gomes, C.M., Brites, D., Fernandes, A., 2018. Impaired oligodendrogenesis and myelination by elevated S100B levels during neurodevelopment. Neuropharmacology 129, 69–83. https://doi.org/10.1016/j.neuropharm.2017.11.002.
Schmuck, G., Mihail, F., 2004. Effects of the carbamates fenoxycarb, propamocarb and propoxur on energy supply, glucose utilization and SH-groups in neurons. Arch. Toxicol. 78 (6), 330–337. https://doi.org/10.1007/s00204-004-0546-3.
Seibenhener, M.L., Wooten, M.W., 2012. Isolation and culture of hippocampal neurons from prenatal mice. J. Vis. Exp.(65). https://doi.org/10.3791/3634.
Seth, B., Yadav, A., Agarwal, S., Tiwari, S.K., Chaturvedi, R.K., 2017. Inhibition of the transforming growth factor-beta/SMAD cascade mitigates the anti-neurogenic effects of the carbamate pesticide carbofuran. J. Biol. Chem. 292 (47), 19423–19440. https://doi.org/10.1074/jbc.M117.798074.
Simons, M., Nave, K.A., 2015. Oligodendrocytes: myelination and axonal support. Cold Spring Harb. Perspect. Biol. 8 (1), a020479. https://doi.org/10.1101/cshperspect.a020479.
Sozmen, E.G., Rosenzweig, S., Llorente, I.L., DiTullio, D.J., Machnicki, M., Vinters, H.V., Havton, L.A., Giger, R.J., Hinman, J.D., Carmichael, S.T., 2016. Nogo receptor blockade overcomes remyelination failure after white matter stroke and stimulates functional recovery in aged mice. Proc. Natl. Acad. Sci. U. S. A. 113 (52), E8453–E8462. https://doi.org/10.1073/pnas.1615322113.
Takeda, M., Nelson, D.J., Soliven, B., 1995. Calcium signaling in cultured rat oligodendrocytes. Glia 14 (3), 225–236. https://doi.org/10.1002/glia.440140308.
Tiwari, S.K., Agarwal, S., Seth, B., Yadav, A., Nair, S., Bhatnagar, P., Karmakar, M., Kumari, M., Chauhan, L.K., Patel, D.K., Srivastava, V., Singh, D., Gupta, S.K., Tripathi, A., Chaturvedi, R.K., Gupta, K.C., 2014. Curcumin-loaded nanoparticles potently induce adult neurogenesis and reverse cognitive deficits in Alzheimer's disease model via canonical Wnt/beta-catenin pathway. ACS Nano 8 (1), 76–103. https://doi.org/10.1021/nn405077y.
Tiwari, S.K., Agarwal, S., Chauhan, L.K., Mishra, V.N., Chaturvedi, R.K., 2015a. Bisphenol-A impairs myelination potential during development in the hippocampus of the rat brain. Mol. Neurobiol. 51 (3), 1395–1416. https://doi.org/10.1007/s12035-014-8817-3.
Tiwari, S.K., Agarwal, S., Seth, B., Yadav, A., Ray, R.S., Mishra, V.N., Chaturvedi, R.K., 2015b. Inhibitory effects of bisphenol-A on neural stem cells proliferation and differentiation in the rat brain are dependent on Wnt/beta-catenin pathway. Mol. Neurobiol. 52 (3), 1735–1757. https://doi.org/10.1007/s12035-014-8940-1.
Tiwari, S.K., Seth, B., Agarwal, S., Yadav, A., Karmakar, M., Gupta, S.K., Choubey, V., Sharma, A., Chaturvedi, R.K., 2015c. Ethosuximide induces hippocampal neurogenesis and reverses cognitive deficits in an amyloid-beta toxin-induced Alzheimer rat model via the phosphatidylinositol 3-kinase (PI3K)/Akt/Wnt/beta-catenin pathway. J. Biol. Chem. 290 (47), 28540–28558. https://doi.org/10.1074/jbc.M115.652586.
Vitry, S., Avellana-Adalid, V., Hardy, R., Lachapelle, F., Baron-Van Evercooren, A., 1999. Mouse oligospheres: from pre-progenitors to functional oligodendrocytes. J. Neurosci. Res. 58 (6), 735–751.
Vrolyk, V., Haruna, J., Benoit-Biancamano, M.O., 2018. Neonatal and juvenile ocular development in Sprague-Dawley rats: a histomorphological and immunohistochemical study. Vet. Pathol. 55 (2), 310–330. https://doi.org/10.1177/0300985817738098.
Wang, J., Pol, S.U., Haberman, A.K., Wang, C., O'Bara, M.A., Sim, F.J., 2014. Transcription factor induction of human oligodendrocyte progenitor fate and differentiation. Proc. Natl. Acad. Sci. U. S. A. 111 (28), E2885–2894. https://doi.org/10.1073/pnas.1408295111.
Wang, H., Wu, M., Zhan, C., Ma, E., Yang, M., Yang, X., Li, Y., 2012. Neurofilament proteins in axonal regeneration and neurodegenerative diseases. Neural Regen. Res. 7

(8), 620–626. https://doi.org/10.3969/j.issn.1673-5374.2012.08.010.
Wegener, A., Deboux, C., Bachelin, C., Frah, M., Kerninon, C., Seilhean, D., Weider, M., Wegner, M., Nait-Oumesmar, B., 2015. Gain of Olig2 function in oligodendrocyte progenitors promotes remyelination. Brain 138 (Pt. 1), 120–135. https://doi.org/10.1093/brain/awu375.
Wischhof, L., Irrsack, E., Osorio, C., Koch, M., 2015. Prenatal LPS-exposure–a neurodevelopmental rat model of schizophrenia-differentially affects cognitive functions, myelination and parvalbumin expression in male and female offspring. Prog. Neuropsychopharmacol. Biol. Psychiatry 57, 17–30. https://doi.org/10.1016/j.pnpbp.2014.10.004.
Young, K.M., Psachoulia, K., Tripathi, R.B., Dunn, S.J., Cossell, L., Attwell, D., Tohyama, K., Richardson, W.D., 2013. Oligodendrocyte dynamics in the healthy adult CNS: evidence for myelin remodeling. Neuron 77 (5), 873–885. https://doi.org/10.1016/j.neuron.2013.01.006.
Zhang, J., Zhang, Y., Dutta, D.J., Argaw, A.T., Bonnamain, V., Seto, J., Braun, D.A., Zameer, A., Hayot, F., Lopez, C.B., Raine, C.S., John, G.R., 2011. Proapoptotic and antiapoptotic actions of Stat1 versus Stat3 underlie neuroprotective and immunoregulatory functions of IL-11. J. Immunol. 187 (3), 1129–1141. https://doi.org/10.4049/jimmunol.1004066.
Zhang, Y., Argaw, A.T., Gurfein, B.T., Zameer, A., Snyder, B.J., Ge, C., Lu, Q.R., Rowitch, D.H., Raine, C.S., Brosnan, C.F., John, G.R., 2009. Notch1 signaling plays a role in regulating precursor differentiation during CNS remyelination. Proc. Natl. Acad. Sci. U. S. A. 106 (45), 19162–19167. https://doi.org/10.1073/pnas.0902834106.